Title

High fat intake sustains sorbitol intolerance after antibiotic-mediated Clostridia depletion from the gut microbiota

Journal

Cell, 187(5)

ISSN

0092-8674

Authors

Lee, Jee-Yon

Tiffany, Connor R

Mahan, Scott P

et al.

Publication Date

2024-02-01

DOI

10.1016/j.cell.2024.01.029

Cell

High fat intake sustains sorbitol intolerance after antibiotic-mediated *Clostridia* depletion from the gut microbiota

Graphical abstract

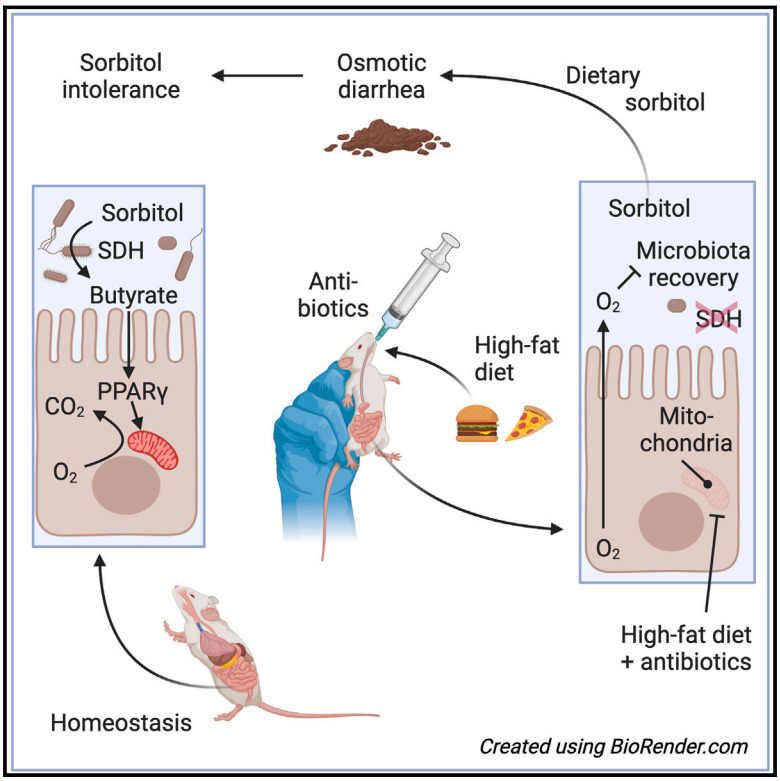

Highlights

- Low fecal SDH is a potential biomarker for sorbitol intolerance
- High fat intake after antibiotics impairs microbiota recovery to lower fecal SDH level
- Abundant sorbitol-consuming probiotics deplete sorbitol to protect against intolerance
- Activating epithelial mitochondria promotes microbiota recovery to rise fecal SDH levels

Authors

Jee-Yon Lee, Connor R. Tiffany, Scott P. Mahan, ..., Emiley A. Eloe-Fadrosh, Peter J. Turnbaugh, Andreas J. Bäumler

Correspondence

ajbaumler@ucdavis.edu

In brief

A history of antibiotics in mice on a high-fat diet triggered sorbitol intolerance by reducing *Clostridia* abundance, which could be treated with abundant sorbitol-consuming probiotics.

Lee et al., 2024, Cell *187*, 1191–1205
February 29, 2024
https://doi.org/10.1016/j.cell.2024.01.029

CellPress

Cell

CellPress
OPEN ACCESS

Article

High fat intake sustains sorbitol intolerance after antibiotic-mediated *Clostridia* depletion from the gut microbiota

Jee-Yon Lee,[1] Connor R. Tiffany,[1] Scott P. Mahan,[1] Matthew Kellom,[2] Andrew W.L. Rogers,[1] Henry Nguyen,[1] Eric T. Stevens,[3] Hugo L.P. Masson,[1] Kohei Yamazaki,[1,4] Maria L. Marco,[3] Emiley A. Eloe-Fadrosh,[2] Peter J. Turnbaugh,[5,6] and Andreas J. Bäumler[1,7,*]

[1]Department of Medical Microbiology and Immunology, School of Medicine, University of California at Davis, One Shields Ave, Davis, CA 95616, USA
[2]Environmental Genomics & Systems Biology Division, Lawrence Berkeley National Laboratory, Berkeley, CA 94720, USA
[3]Department of Food Science and Technology, University of California at Davis, Davis, CA 95616, USA
[4]Laboratory of Veterinary Public Health, School of Veterinary Medicine, Kitasato University, Towada, Japan
[5]Department of Microbiology & Immunology, University of California, San Francisco, San Francisco, CA 94143, USA
[6]Chan Zuckerberg Biohub-San Francisco, San Francisco, CA 94158, USA
[7]Lead contact
*Correspondence: ajbaumler@ucdavis.edu
https://doi.org/10.1016/j.cell.2024.01.029

SUMMARY

Carbohydrate intolerance, commonly linked to the consumption of lactose, fructose, or sorbitol, affects up to 30% of the population in high-income countries. Although sorbitol intolerance is attributed to malabsorption, the underlying mechanism remains unresolved. Here, we show that a history of antibiotic exposure combined with high fat intake triggered long-lasting sorbitol intolerance in mice by reducing *Clostridia* abundance, which impaired microbial sorbitol catabolism. The restoration of sorbitol catabolism by inoculation with probiotic *Escherichia coli* protected mice against sorbitol intolerance but did not restore *Clostridia* abundance. Inoculation with the butyrate producer *Anaerostipes caccae* restored a normal *Clostridia* abundance, which protected mice against sorbitol-induced diarrhea even when the probiotic was cleared. Butyrate restored *Clostridia* abundance by stimulating epithelial peroxisome proliferator-activated receptor-gamma (PPAR-γ) signaling to restore epithelial hypoxia in the colon. Collectively, these mechanistic insights identify microbial sorbitol catabolism as a potential target for approaches for the diagnosis, treatment, and prevention of sorbitol intolerance.

INTRODUCTION

Sorbitol is a naturally occurring polyol that is poorly absorbed by the small intestine, resulting in a low caloric content. Therefore, sorbitol is used as low-calorie sweetener in "sugar-free" foods, such as sugar-free chewing gum, candy, mints, jam, diet drinks, and chocolate.[1] The estimated daily sorbitol intake in the UK averages 3.5 g,[2] which comes mostly from its use as sweetener, but sorbitol is also naturally present at low concentrations in some fruits of the *Rosaceae* family, such as apples, pears, and apricots.[3] Excessive consumption of polyols can trap fluid in the colonic lumen to trigger osmotic diarrhea.[4] For example, ingestion of 20 g sorbitol can induce symptoms of carbohydrate intolerance in healthy volunteers, including diarrhea, abdominal distention, and flatulence, but most volunteers ingesting 5 g sorbitol do not develop such symptoms.[5] Susceptibility to polyol-induced diarrhea varies among individuals, resulting in heightened intolerance in patients with irritable bowel syndrome (IBS)[6,7] or quiescent inflammatory bowel disease (IBD).[8,9] For example, ingesting 5 g of sorbitol can intensify gastrointestinal symptoms in individuals with IBS,[10] whereas consuming 3 g of sorbitol can exacerbate gastrointestinal symptoms in IBD patients.[11]

Antibiotic treatment can transiently heighten polyol intolerance by disrupting the gut microbiota, which can impair metabolic functions that remove osmotically active solutes.[12,13] In a mouse model of antibiotic-induced sorbitol intolerance, the addition of 5% sorbitol to the drinking water increases fecal water content during treatment with ampicillin or streptomycin (Str), but not in the absence of antibiotic treatment.[14] However, antibiotic-induced changes in the microbiota composition are short lived, as the gut microbiota regains its normal composition within 5 days after withdrawing Str.[15–17] Since polyol intolerance resolves as the microbiota recovers after antibiotic treatment,[18] a transient disruption of the microbiota by antibiotics does not explain the prolonged carbohydrate intolerance in patients with

IBS or quiescent IBD.[6–9] Treatment of prolonged polyol intolerance therefore relies on dietary interventions that reduce the intake of polyols and other poorly absorbed mono-, di-, and oligosaccharides.[19]

A recent history of antibiotic usage (between 4 and 56 weeks prior to enrollment) in combination with high fat intake is an environmental risk factor in adult patients for developing diarrhea, abdominal distention, and flatulence.[20] These individuals can be differentiated from IBS patients by their elevated fecal calprotectin levels (between 50 and 200 μg/g feces), which is a marker of intestinal inflammation. However, intestinal inflammation in these individuals does not rise to the level of IBD, which is characterized by fecal calprotectin levels exceeding 250 μg/g feces during active disease.[21] Patients with low grade mucosal inflammation that is associated with a history of antibiotics and high fat intake thus represents a syndrome located at the intersection of the clinical spectra of IBS and IBD.[22–24] Elevated fecal calprotectin levels and diarrhea observed in these patients can be recapitulated in mice exposed to high fat intake in combination with a history of Str treatment.[20] When antibiotics are combined with maintaining mice on a high-fat (HF) diet, microbiota recovery is impaired even 4 weeks after Str treatment, as indicated by increased *Enterobacterales* (ord. nov.,[25] phylum *Proteobacteria*) and reduced *Clostridia* (phylum *Firmicutes*) abundance. These changes in the microbiota composition match those in the feces of patients with a history of antibiotics and high fat intake,[20] and in IBD patients.[26–28] As mice with a history of antibiotic treatment and high fat intake recapitulate signs of disease seen in patients with diarrhea, abdominal distention, and flatulence, we wanted to investigate whether exposure to these environmental risk factors creates a mouse model for prolonged sorbitol intolerance that can be used to explore approaches for diagnosis, treatment, and prevention.

RESULTS

Str induces sorbitol intolerance that resolves within 5 days after treatment

First, we wanted to investigate how quickly sorbitol intolerance resolves after cessation of antibiotic treatment. Mice (C57BL/6J) fed a low-fat (LF) diet (10% fat) were mock-treated or treated with a single dose of Str. Subsequently, mice received drinking water without supplementation or drinking water supplemented with 5% sorbitol for 2 days to assess sorbitol tolerance. When supplementation of drinking water with 5% sorbitol was started 1 day after Str treatment, it resulted in increased fecal water content in Str-treated mice, but not in mock-treated control animals (Figure S1A). Furthermore, antibiotic treatment exacerbated weight loss during sorbitol supplementation, and a humane endpoint (20% weight loss) was reached for some animals by the second day of sorbitol supplementation (Figure S1B). However, when supplementation with 5% sorbitol was started 5 days after Str treatment, signs of sorbitol intolerance were no longer observed (Figures S1C and S1D). Concentrations of sorbitol in the cecal contents were elevated when sorbitol supplementation was started 1 day after Str treatment, which indicated that the solute accumulates in the lumen of the large intestine when the microbiota is disrupted. However, concentrations of sorbitol in the cecal contents were no longer elevated when sorbitol supplementation commenced 5 days after Str treatment (Figure S1E), when the microbiota regains a normal composition.[15–17] Thus, our data suggested that transient sorbitol intolerance was correlated with an antibiotic-mediated disruption of the gut microbiota.

Combining antibiotic exposure with HF diet drives prolonged sorbitol intolerance

Our previous work shows that microbiota recovery is impaired when exposure to Str is combined with high fat intake.[20] We thus wanted to determine whether exposure to this combination of environmental factors would result in prolonged sorbitol intolerance. Mice (C57BL/6J) reared and maintained throughout the experiment on a LF diet (10% fat) or a HF diet (45% fat) were mock-treated or received a single dose of Str by oral gavage to generate a history of antibiotic usage, respectively. 4 weeks later, mice were considered to have a "history" of antibiotic treatment and received drinking water supplemented with 5% sorbitol for 3 days. Combining Str treatment with high fat intake produced signs of sorbitol intolerance, including weight loss (Figure 1A), increased fecal water content (Figure 1B), and elevated sorbitol levels in cecal contents (Figure 1C), even 4 weeks after antibiotic exposure. Supplementation with sorbitol for 3 days did not alter water intake (Figure S1F) or signs of inflammation, as assessed by measuring colon length (Figure S1G). Importantly, HF diet alone did not produce signs of sorbitol intolerance, such as weight loss (Figure S1H), increased fecal water content (Figure S1I), or elevated sorbitol levels in cecal contents (Figure S1J).

Reduced SDH activity is a potential biomarker for sorbitol intolerance

We wanted to determine whether sorbitol intolerance is associated with reduced activity of sorbitol dehydrogenase (SDH) (officially designated L-iditol 2-dehydrogenase), the enzyme catalyzing the conversion of sorbitol into sorbose or fructose. Mice with a history of antibiotic treatment and high fat intake featured reduced SDH activity in cecal extracts (Figure 1D).

Next, we explored whether reduced fecal SDH activity is also a biomarker observed in patients. Combining a history of Str treatment with high fat intake provides an animal model for patients complaining about diarrhea, abdominal distention, and flatulence, who have a recent history of antibiotic usage and report higher fat intake than healthy controls and patients with IBS.[20] Fecal samples banked from this previous study were analyzed for fecal SDH activity. Notably, patients with elevated fecal calprotectin had decreased fecal SDH activity compared with IBS patients or healthy controls (Figure 1E). In a questionnaire, patients with low fecal SDH activity were more likely to indicate that they experienced gastrointestinal symptoms associated with consumption of sugar-free food or beverages (Figure 1F). Collectively, these data identify low fecal SDH activity as a potential biomarker for prolonged sorbitol intolerance.

Str exposure combined with high fat intake depletes the classes *Clostridia*, *Betaproteobacteria*, and *Actinobacteria*

Next, we wanted to determine which bacterial taxa protect against sorbitol intolerance during homeostasis. To analyze

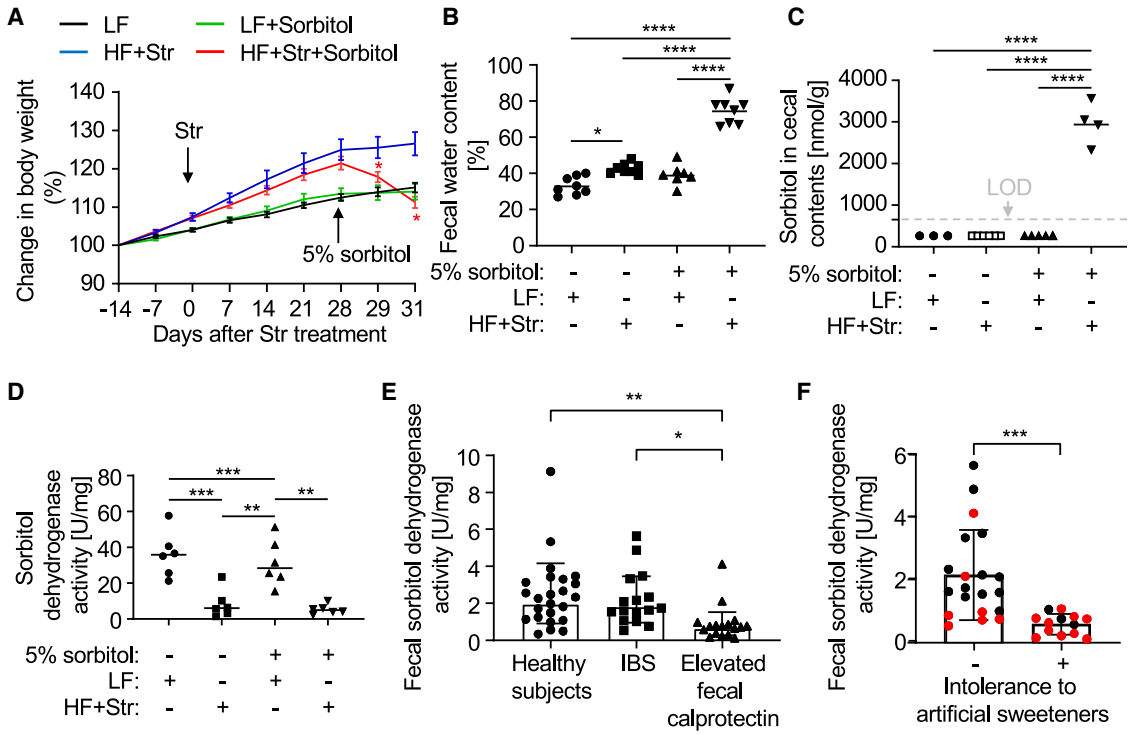

Figure 1. Mouse model of prolonged sorbitol intolerance

Mice maintained on a low-fat (LF) diet or a high-fat (HF) diet for 14 days were mock-treated or received a single dose of streptomycin (Str) by oral gavage. After maintaining mice for 4 more weeks on the same diet, mice received drinking water supplemented with 5% sorbitol for 3 days.

(A) Change in body weight for each group (n = 14) over time.

(B) Fecal water content after 3 days of sorbitol supplementation.

(C) Sorbitol concentration after 3 days of sorbitol supplementation. LOD, limit of detection.

(D) Sorbitol dehydrogenase activity in cecal contents. (B–D) Group sizes (n) are indicated by the number of symbols. *p < 0.05; **p < 0.01; ***p < 0.005; ****p < 0.001. (A, B, and F) Analysis with two-way (A) or one-way (B–E) ANOVA followed by Tukey's multiple-comparison test (A), or Student's t test (F). (A, E, and F) Error bars indicate standard deviation.

See also Figure S1.

changes in the microbiota composition, fecal samples collected from the experiment shown in Figures 1A–1D prior to antibiotic treatment (day 0; homeostasis) and 4 weeks after antibiotic treatment (day 28; sorbitol intolerance) (Figure S2A) were analyzed by 16S ribosomal RNA gene amplicon sequencing (microbiota profiling) (Figure S2B). Consistent with previous results,[20] prior Str treatment and high fat intake significantly reduced the relative abundance of amplicon sequence variants (ASVs) belonging to the class *Clostridia* (Figure 2A). A history of antibiotic treatment and high fat intake increased the abundance of ASVs belonging to the classes *Bacilli*, *Bacteroidia*, or *Verrucomicrobiae* in some animals (Figures S2B and S2C). In mice with a history of antibiotic exposure and high fat intake, the most notable increase in the relative abundance was observed for ASVs belonging to the genus *Enterococcus* (class *Bacilli*). The microbiota composition varied between animals from this group (Figure 2B), but variability could not be explained by cage effects. Linear discriminant analysis of fecal samples prior to, and 4 weeks after Str treatment revealed that prior Str treatment combined with high fat intake significantly increased several ASVs within the class *Bacilli* and significantly reduced the relative abundances of the classes *Clostridia*, *Betaproteobacteria*, and *Actinobacteria* (Figure 2C).

Metagenomic analysis identifies *Clostridia* as the main source of genes involved in sorbitol catabolism during homeostasis

We next wanted to determine which of the taxa that were depleted in mice with sorbitol intolerance were likely to prevent sorbitol intolerance during homeostasis. To analyze the metabolic capacity of the microbiota, we performed shotgun metagenomic sequencing on fecal samples collected from the experiment shown in Figures 1A–1D prior to antibiotic treatment (homeostasis) or 4 weeks after antibiotic treatment (sorbitol intolerance) (Figure S2A).

Metagenomic analysis identified a total of 11,979 unique genes from medium to high-quality binned genomes (bins), which were annotated using the Kyoto Encyclopedia of Genes and Genomes (KEGG) brite orthology database.[29] Since this study focused on carbohydrate metabolism, our analysis remained focused on a small subset of unique genes. However, to allow readers to explore data regarding genes not related to carbohydrate catabolism, we developed a web application that allows interactive analysis of all KEGG orthology pathways within the dataset (https://clostridia-enjoyer.shinyapps.io/sorbitolMetagenome/). Metagenomic analysis identified 421

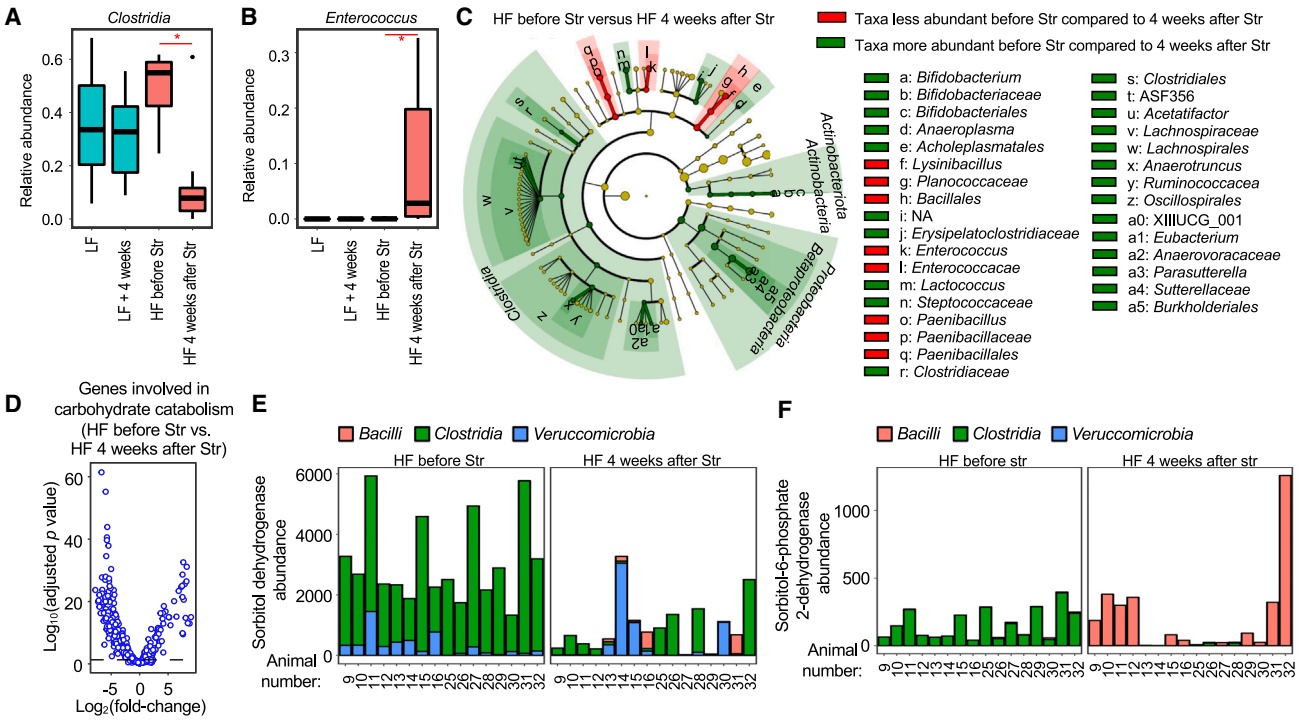

Figure 2. *Clostridia* are a main source of sorbitol dehydrogenase genes during homeostasis

Mice were maintained on a low-fat (LF) diet or a high-fat (HF) diet for 14 days. Fecal samples were collected ("LF" or "HF before Str"), and mice were mock-treated or received a single dose of streptomycin (Str) by oral gavage. After maintaining mice for 4 more weeks on the same diet, a second fecal sample was collected for analysis ("LF + 4 weeks" or "HF 4 weeks after Str").

(A–C) Microbiota profiling of fecal DNA collected at the indicated time points. (A and B) Relative abundance of amplicon sequence variants (ASVs) belonging to the class *Clostridia* (A) or the genus *Enterococcus* (B). Boxplots represent the first to third quartiles, and lines indicate median values. *$p < 0.05$. Analysis with Kruskal-Wallis test. (C) The cladogram shows differences in taxa composition between samples collected before streptomycin treatment (HF before Str) and 4 weeks after streptomycin treatment (HF 4 weeks after Str). Taxa that are significantly (Kruskal-Wallis test, linear discriminant analysis effect size [LEfSe]) more abundant (green) or less abundant (red) before compared with 4 weeks after streptomycin treatment are shown.

(D–F) DNA isolated from the indicated samples was subjected to metagenomic analysis. (D) Volcano plot of genes involved in carbohydrate metabolism. Negative values indicate genes with decreased abundance 4 weeks after streptomycin treatment compared with prior to streptomycin treatment. (E and F) Abundance of genes encoding sorbitol dehydrogenase (E) or sorbitol-6-phosphate 2-dehydrogenase (F) in samples collected prior to or 4 weeks after streptomycin treatment. See also Figures S2, S3, S4, and S5.

genes involved in carbohydrate catabolism. Hierarchical clustering of samples using the 421 genes belonging to carbohydrate metabolism revealed 3 distinct clusters. One cluster contained samples collected before Str treatment, while the other 2 clusters contained samples 4 weeks after Str treatment (Figure S3). Differential abundance analysis of genes involved in carbohydrate metabolism revealed more significantly decreased genes than increased genes 4 weeks after Str treatment (Figure 2D). Among the genes with significantly reduced abundance after exposure to environmental risk factors were those involved in the catabolism of polyols, including mannitol, galactitol, erythritol, ribitol, and arabinitol (Figure S4A).

Two pathways for sorbitol catabolism have been described in bacteria. The first pathway involves transport across the bacterial cytoplasmic membrane through an ATP binding cassette (ABC) transporter[30] or a transport system of the major facilitator superfamily (MFS).[31] Transport of sorbitol into the cytosol is then followed by an NAD^+-dependent conversion into either sorbose or fructose by SDH. Genes encoding SDH activity form a distinct subfamily within the polyol dehydrogenase family.[32] The majority of SDH encoding reads from medium and high-quality bins in samples collected prior to antibiotic treatment were derived from bins belonging to the class *Clostridia* (Figure 2E). A history of antibiotic treatment and high fat intake significantly reduced the abundance of SDH encoding reads (Figures 2E and S2D).

The second pathway for sorbitol utilization involves transport across the bacterial cytoplasmic membrane through a phosphotransferase (PTS) system, which is coupled to a phosphoenolpyruvate-dependent phosphorylation of sorbitol to yield sorbitol-6-phosphate. The enzyme sorbitol-6-phosphate 2-dehydrogenase then catalyzes the cytosolic conversion of sorbitol-6-phosphate and NAD^+ to fructose-6-phosphate, NADH, and H^+. The main source of sorbitol-6-phosphate 2-dehydrogenase encoding reads in samples collected prior to antibiotic treatment was from bins belonging to the class *Clostridia* (Figure 2F). By contrast, the majority of sorbitol-6-phosphate 2-dehydrogenase encoding reads collected 4 weeks after Str treatment of mice on a HF diet were derived from bins belonging to the class *Bacilli*. However, the overall relative abundance of sorbitol-6-phosphate 2-dehydrogenase encoding reads did not

significantly change between treatment groups (Figure S2D). Overall, SDH encoding reads were more abundant than sorbitol-6-phosphate 2-dehydrogenase encoding reads (Figures 2E and 2F), suggesting that the former might be the dominate pathway for removal of sorbitol from the intestinal lumen during homeostasis.

The majority of SDH and sorbitol-6-phosphate 2-dehydrogenase encoding reads in samples collected prior to antibiotic exposure were derived from bins belonging to the class *Clostridia* (Figures 2E and 2F) and the order *Lachnospirales* (class *Clostridia*) (Figure S2E). A history of antibiotic treatment and high fat intake reduced the abundance of *Clostridia*, which made *Bacilli* and *Verrucomicrobiae* the most prominent sources of genes involved in sorbitol catabolism. However, an increased abundance of SDH encoding reads from *Bacilli* and *Verrucomicrobiae* did not fully compensate for the loss of SDH encoding reads from *Clostridia*, thus reducing the overall metabolic potential to catabolize sorbitol in microbial communities from mice with a history of antibiotic treatment and high fat intake (Figure 2E).

Diminished microbial sorbitol catabolism causes sorbitol intolerance

To directly test whether impairment of microbial sorbitol catabolism causes sorbitol intolerance, we used *Escherichia coli* strain Nissle 1917 (family *Enterobacteriaceae*), a genetically tractable probiotic that catabolizes sorbitol.[33] To facilitate engraftment of the probiotic, we initially used a model of transient sorbitol intolerance (Figure S1) in which disruption of the gut microbiota with Str ensures efficient colonization. Mice reared and maintained throughout the experiment on a LF diet were inoculated 1 day after Str treatment with different doses (between 10^0 and 10^9 colony-forming units [CFUs] per animal) of *E. coli* strain Nissle 1917 to generate mice that differed in their absolute *E. coli* abundance in the feces (Figures 3A and 3B). At the day of inoculation with *E. coli* Nissle 1917, supplementation of drinking water with 5% sorbitol was started. Supplementation of drinking water with 5% sorbitol for 2 days produced sorbitol-induced diarrhea (Figure 3C) in Str-treated mice that carried *E. coli* Nissle 1917 below a threshold of 10^8 CFU/g feces (Figure 3A) or 10^6 16S rRNA gene copies/20 ng DNA (Figure 3B). By contrast, mock-treated mice or Str-treated mice that carried *E. coli* Nissle 1917 above threshold levels were protected from sorbitol-induced diarrhea (Figures 3A–3C). Cecal SDH activity was reduced by treatment with Str but was restored when mice were colonized with *E. coli* at levels above the threshold (Figure 3D).

To test whether the ability of *E. coli* to protect against sorbitol intolerance was dependent on its ability to ferment sorbitol, we constructed a mutant deficient for sorbitol catabolism (*srlAEB* mutant). Whereas *E. coli* Nissle 1917 was able to deplete sorbitol in aerobic broth culture, a *srlAEB* mutant was no longer able to catabolize this sugar *in vitro*. Sorbitol fermentation could be restored in a *srlAEB* mutant by introducing the *srlAEB* genes on a plasmid (pAWLR196) but not by introducing an empty vector control (pWSK29) (Figure 3E). Notably, the ability of *E. coli* to protect against sorbitol-induced diarrhea *in vivo* was dependent on its ability to ferment sorbitol, because protection was no longer observed (Figure 3F) in Str-treated mice colonized above threshold levels with an *E. coli* strain deficient for sorbitol catabolism (*srlAEB* mutant) (Figure 3G). These data provided genetic evidence to causatively linked sorbitol intolerance to an impairment of microbial sorbitol catabolism.

Assignment of most reads involved in sorbitol catabolism to *Clostridia* bins during homeostasis (Figures 2E and 2F) suggested that a lasting depletion of this taxon (Figure 2A) triggers sorbitol intolerance. We thus explored whether a sorbitol-consuming member of the class *Clostridia* could serve as a second-generation probiotic[35] to treat sorbitol intolerance. *Anaerostipes caccae* is a commensal, butyrate-producing *Clostridia* isolate[36] that can utilize sorbitol as a sole carbon source *in vitro* (Figure 3H).[34] *A. caccae* was neither detected by microbiota profiling nor by metagenomic analysis in microbiota of mice analyzed in this study, but this species is prevalent and abundant in the human fecal microbiota.[37,38] In a proof-of-concept experiment, mice (C57BL/6J) reared and maintained throughout the experiment on a LF diet were mock-treated or treated with a single dose of Str to generate transient sorbitol intolerance and to facilitate colonization. 1 day later, drinking water was supplemented with 5% sorbitol, and groups of Str-treated mice were inoculated with different doses of *A. caccae*. The resulting groups of Str-treated mice differed in their absolute abundance of *A. caccae* in the feces (Figure 3I). Supplementation of drinking water with 5% sorbitol for 2 days produced signs of sorbitol-induced diarrhea (Figure 3J) in Str-treated mice that carried *A. caccae* below a threshold of approximately 10^6 16S rRNA gene copies/20 ng DNA (Figure 3I), which was similar to the threshold determined for *E. coli* (Figure 3B). The SDH activity of the microbiota was reduced by treatment with Str but was restored when mice were colonized with *A. caccae* at levels above the threshold (Figure 3K).

Treatment of prolonged sorbitol intolerance with sorbitol-catabolizing probiotics

We next wanted to test whether treatment with sorbitol-consuming probiotics would protect against prolonged sorbitol intolerance. Mice reared and maintained throughout the experiment on a LF or a HF diet were mock-treated or received a single dose of Str, respectively. 4 weeks later, mice received drinking water supplemented with 5% sorbitol and were inoculated with 10^9 CFUs of *E. coli* Nissle 1917, *A. caccae*, or *Lactiplantibacillus plantarum* strain NICMB8826-R (class *Bacilli*, phylum *Firmicutes*), a probiotic strain that can catabolize sorbitol (Figure 4A). After 3 days of sorbitol supplementation, all three probiotics conferred protection against sorbitol-induced diarrhea (Figure 4B). Whereas the degree of protection against sorbitol-induced diarrhea afforded by *A. caccae* and *E. coli* Nissle 1917 did not change over time, *L. plantarum* no longer conferred protection after 7 days of sorbitol supplementation. All three probiotics prevented accumulation of sorbitol in cecal contents after 3 days of supplementation, but sorbitol started to accumulate in ceca of mice inoculated with *L. plantarum* after 7 days (Figure 4C). Whereas all three probiotics provided some degree of protection against sorbitol-induced diarrhea, only *A. caccae* lowered fecal water content to levels seen in controls without sorbitol intolerance (Figure 4B).

Since protection against transient sorbitol intolerance requires colonization above a certain threshold (Figures 3A–3C, 3I,

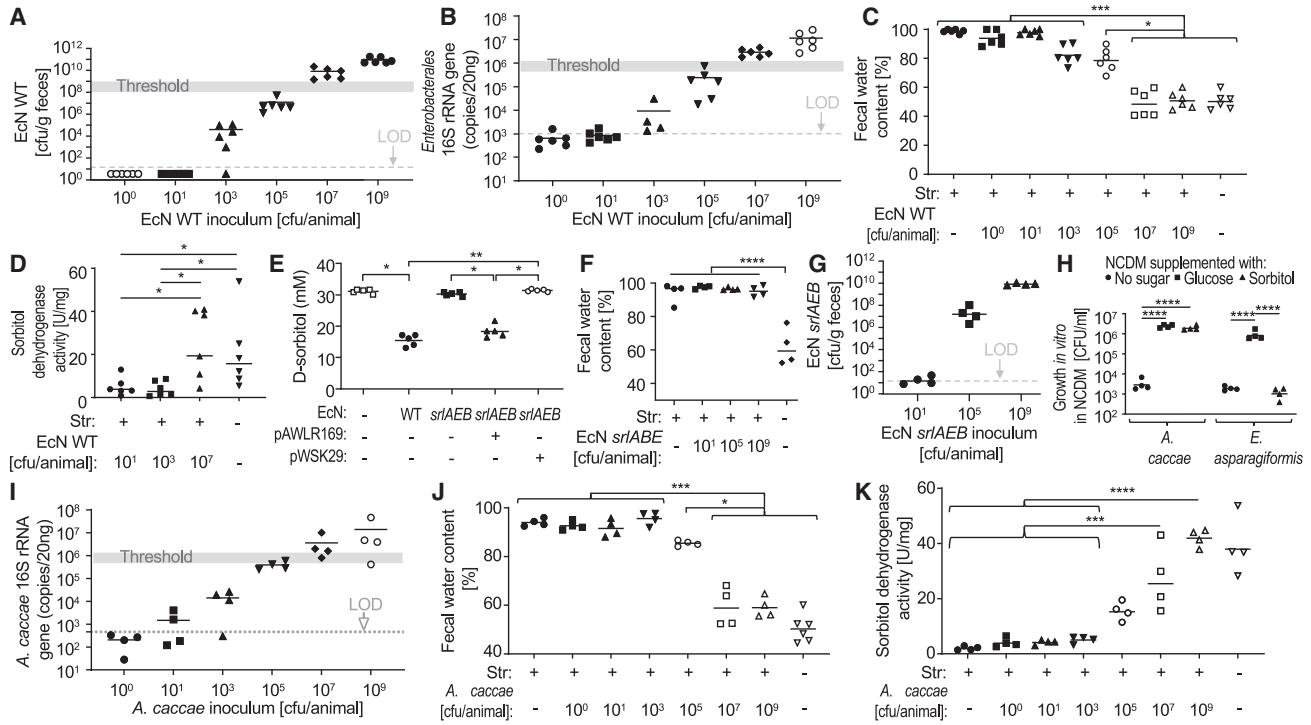

Figure 3. Abundant probiotics protect against transient sorbitol intolerance

(A–D and F–K) Mice were mock-treated or treated with a single dose of streptomycin. 1 day later, drinking water was supplemented with 5% sorbitol, and mice were inoculated with different doses of *E. coli* Nissle 1917 (EcN WT), an *E. coli* Nissle 1917 *srlABE* mutant (EcN *srlABE*), or *A. caccae*. Samples were collected after 2 days of sorbitol supplementation.

(A) Colony-forming units (CFUs) recovered from feces of animals (y axis) 2 days after inoculation with the indicated doses of EcN WT (x axes).

(B) The abundance of *E. coli* in fecal samples was determined by real-time PCR using *Enterobacterales*-specific primers.

(C and J) Fecal water content in fecal pellets (y axis) collected from animals 2 days after inoculation with the indicated doses (x axes) of *E. coli* Nissle 1917 (C) or *A. caccae* (J).

(D) Sorbitol dehydrogenase activity in cecal contents of mice inoculated with the indicated doses of *E. coli* Nissle 1917.

(E) Minimal medium containing sorbitol as a sole carbon source was inoculated with the indicated *E. coli* Nissle 1917 strains carrying either no plasmid, a plasmid encoding the *srlAEB* genes (pAWLR169), or the empty plasmid vector (pWSK29). After overnight culture, the sorbitol concentration in culture supernatants was measured.

(F) Fecal water content in fecal pellets (y axis) collected from animals 2 days after inoculation with the indicated doses of EcN *srlABE* (x axes).

(G) CFU recovered from feces of animals (y axis) 2 days after inoculation with the indicated doses of EcN *srlABE* (x axes).

(H) *In vitro* anaerobic growth of *A. caccae* in no-carbon defined medium (NCDM) supplemented with glucose, sorbitol, or without supplementation (no sugar). *Enterocloster asparagiformis*, a *Clostridia* species that does not ferment sorbitol,[34] was used as a negative control.

(I) The abundance of *A. caccae* in fecal samples was determined by real-time PCR using genus-specific primers.

(K) Sorbitol dehydrogenase activity in cecal contents of mice inoculated with the indicated doses of *A. caccae*.

(A, B, and I) A gray bar indicates the threshold of colonization required for protection against sorbitol-induced diarrhea. (A, B, G, and I) LOD, limit of detection. *p < 0.05; **p < 0.01; ***p < 0.005; ****p < 0.001. (C–F, H, J, and K) Analysis by one-way ANOVA followed by Tukey's multiple-comparison tests.

and 3J), we first considered that sorbitol-consuming probiotics might differ in their ability to protect against prolonged sorbitol intolerance (Figure 4B) because they differed in their ability to colonize mice. Whereas *E. coli* was recovered from feces in similar numbers at three and 7 days after inoculation, both *L. plantarum* and *A. caccae* colonization levels dropped by several orders of magnitude between days 3 and 7 after inoculation (Figures 4D and 4E). Thus, a possible explanation for a loss of protection conferred by *L. plantarum* 7 days after inoculation (Figure 4B) was that the probiotic was beginning to be cleared (Figure 4D).

The consistently high colonization levels of *E. coli* Nissle 1917 throughout the experiment (Figure 4D) suggested that the probiotic was able to catabolize sorbitol to confer protection throughout the 7-day exposure to sorbitol (Figure 4B). To test whether protection by *E. coli* Nissle 1917 required its ability to catabolize sorbitol, the experiment was repeated with mice inoculated with *E. coli* Nissle 1917 wild-type (WT) or an isogenic sorbitol fermentation-deficient strain (*srlAEB* mutant). 3 days after inoculation, WT and *srlAEB* mutant were recovered in similar numbers from the feces (Figure S6A), but only the sorbitol fermentation-proficient WT depleted sorbitol in cecal contents (Figure S6B) and prevented a rise in fecal water content during sorbitol exposure (Figure S6C). These data suggested that sorbitol catabolism of *E. coli* Nissle 1917 was causatively linked to its ability to protect against prolonged sorbitol intolerance.

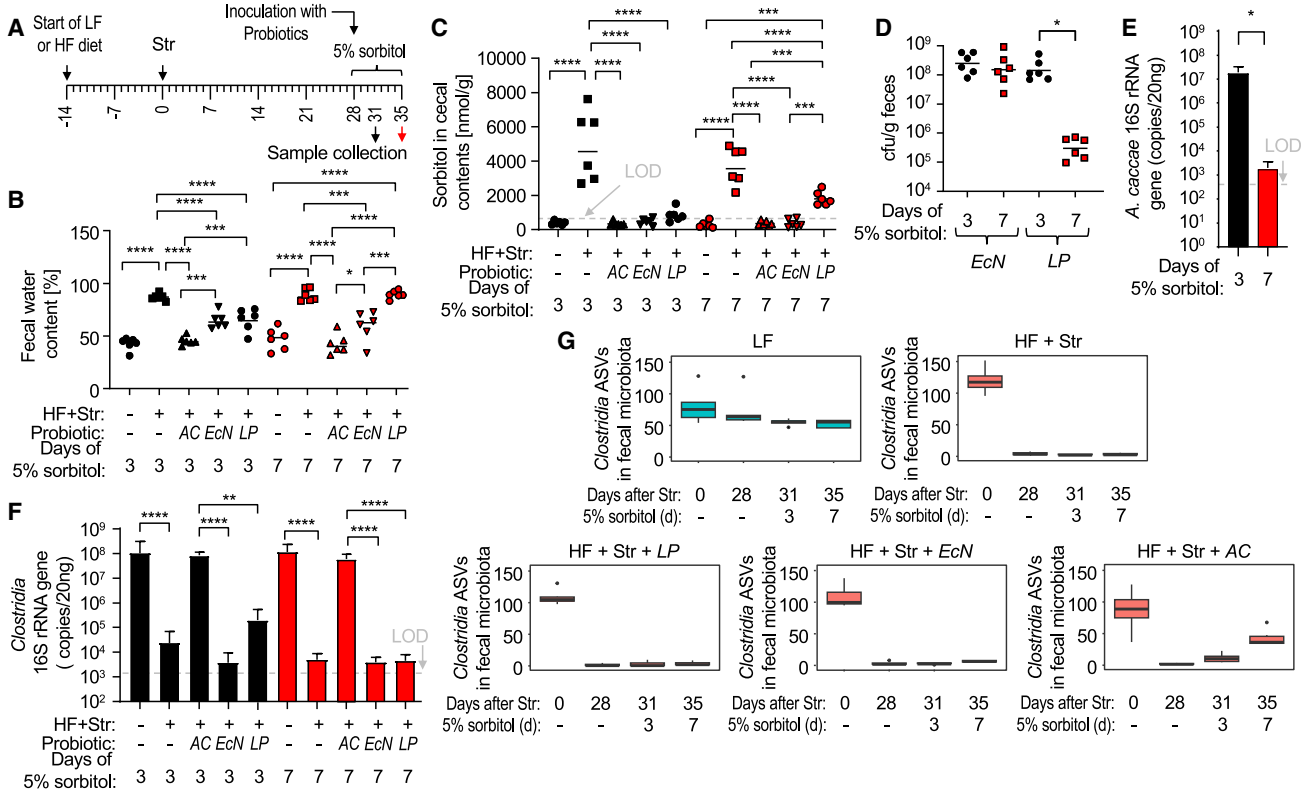

Figure 4. Sorbitol-catabolizing probiotics protect against prolonged sorbitol intolerance

Mice reared and maintained throughout the experiment on a low-fat (LF) or a high-fat (HF) diet were mock-treated or received a single dose of streptomycin (Str), respectively. 4 weeks later, mice received drinking water supplemented with 5% sorbitol and were inoculated with 10^9 colony-forming units (CFUs) of *E. coli* Nissle 1917 (*EcN*), *A. caccae* (*AC*), or *Lactiplantibacillus plantarum* (*LP*). Samples were collected after 3 or 7 days of sorbitol supplementation.

(A) Schematic of experimental groups and time points.

(B) Fecal water content in fecal pellets.

(C) Sorbitol dehydrogenase activity in cecal contents.

(D) CFU of *EcN* or *LP*.

(E) Absolute abundance of *AC* in feces was determined by real-time PCR using genus-specific primers.

(F) Absolute abundance of *Clostridia* in feces determined by real-time PCR using class-specific primers.

(G) Numbers of amplicon sequence variants (ASVs) belonging to the class *Clostridia* at the indicated time points. Box plots represent the first to third quartiles, and lines indicate median values. *p < 0.05; **p < 0.01; ***p < 0.005; ****p < 0.001. Analysis by one-way ANOVA followed by Tukey's multiple-comparison tests (B–D and F) or Student's t test (E). (C, E, and F) LOD, limit of detection. (E and F) Error bars represent standard deviation.

See also Figure S6.

Colonization above threshold levels at 3 days after inoculation (Figures 3I and 4E) suggested that *A. caccae* might protect against sorbitol intolerance at this time point (Figure 4B) by depleting sorbitol (Figure 4C). However, the probiotic still normalized fecal water content after 7 days of sorbitol exposure (Figure 4B), even though *A. caccae* was being cleared by this time point (Figure 4E). Thus, protection conferred by *A. caccae* at 7 days after inoculation (Figure 4B) could not be attributed to its ability to catabolize sorbitol.

Treatment with a butyrate-producing probiotic promotes microbiota recovery

We next investigated whether *A. caccae* protected mice from sorbitol intolerance at 7 days after inoculation because this probiotic promoted an increase in the abundance of other *Clostridia* species, thereby restoring sorbitol catabolism of the microbiota to normal levels. Consistent with this idea, inoculation with *A. caccae* restored a normal absolute abundance of *Clostridia* as indicated by real-time PCR using class-specific primers (Figure 4F), which persisted even after the probiotic had been cleared 7 days after inoculation (Figure 4E). Furthermore, *A. caccae* promoted a rise in *Clostridia* richness, as indicated by detecting increasing numbers of distinct ASVs belonging to the class *Clostridia* during microbiota profiling at 7 days after inoculation with the probiotic (Figure 4G). By contrast, the absolute abundance and richness of the *Clostridia* population remained low in mice treated with *E. coli* Nissle 1917 or *L. plantarum* (Figures 4F and 4G).

One feature that distinguishes *A. caccae* from *E. coli* or *L. plantarum* is its ability to produce the short-chain fatty acid butyrate.[36] We thus wanted to determine whether butyrate production is linked to microbiota recovery. Our metagenomic

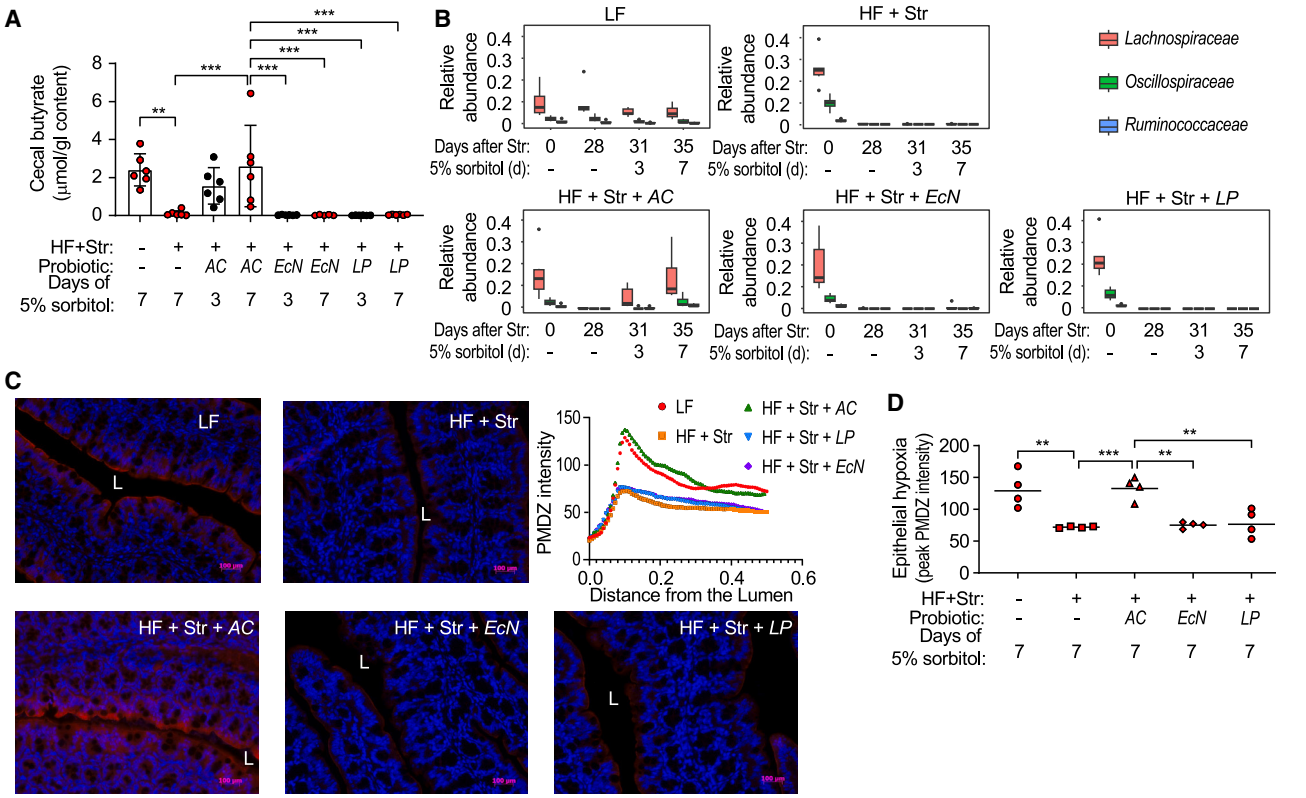

Figure 5. *A. caccae* restores butyrate levels and epithelial hypoxia in mice with prolonged sorbitol intolerance

Mice reared and maintained throughout the experiment on a low-fat (LF) or a high-fat (HF) diet were mock-treated or received a single dose of streptomycin (Str), respectively. 4 weeks later, mice received drinking water supplemented with 5% sorbitol and were inoculated with 10^9 colony-forming units (CFUs) of *E. coli* Nissle 1917 (*EcN*), *A. caccae* (*AC*), or *Lactiplantibacillus plantarum* (*LP*). Samples were collected after 3 or 7 days of sorbitol supplementation.

(A) Butyrate concentrations in cecal contents. Error bars represent standard deviation.

(B) Relative abundance of *Clostridia* families containing gene sequence involved in butyrate metabolism. Box plots represent the first to third quartiles, and lines indicate the median values.

(C and D) Mice were injected with pimonidazole (PMDZ) before euthanasia. PMDZ was detected using hypoxyprobe-1 primary antibody and a Cy-3 conjugated goat anti-mouse secondary antibody (red fluorescence) in colonic sections counter stained with nuclear stain (blue fluorescence). (C) Representative images for each group 7 days after inoculation with probiotics. L, intestinal lumen. The graph shows PMDZ intensity from the lumen across the epithelial layer (distance in arbitrary units). (D) The graph shows the average peak PMDZ intensity. (A and D) Each symbol represent data from one animal. $^{**}p < 0.01$; $^{***}p < 0.005$. Analysis by one-way ANOVA followed by Tukey's multiple-comparison tests (A) or Kruskal-Wallis test (D).

analysis predicted that sorbitol intolerance was linked to a reduced capacity of the microbiota to produce butyrate (Figure S4B). Consistent with this prediction, a history of Str treatment and high fat intake was associated with a marked reduction in the cecal butyrate concentration (Figure 5A). Microbiota profiling revealed that this drop in cecal butyrate levels was linked to a depletion of *Lachnospiraceae* and *Ruminococcaceae* (Figure 5B), two *Clostridia* families that harbor butyrate producers.[39] Treatment with *A. caccae* increased cecal butyrate levels, whereas inoculation with *E. coli* Nissle 1917 or *L. plantarum* did not restore production of this short-chain fatty acid (Figure 5A). Clearance of *A. caccae* by day 7 after inoculation (Figure 4E) suggested that restoration of butyrate levels at this time point (Figure 5A) was likely attributable to an increased abundance of other butyrate-producing species as suggested by an increased abundance of *Lachnospiraceae* (Figure 5B).

Butyrate is a peroxisome proliferator-activated receptor-gamma (PPAR-γ) agonists that maintains epithelial hypoxia in the colon to limit the diffusion of oxygen into the intestinal lumen, which helps maintain anaerobiosis in the lumen.[40] In support of increased oxygen availability in the gut lumen, metagenomic analysis revealed that microbial genes involved in oxidative phosphorylation exhibited an increased abundance after exposure to antibiotics and high fat intake (Figure S5). Consistent with a previous report,[20] a history of Str treatment and high fat intake was associated with a loss of epithelial hypoxia (Figures 5C and 5D). Notably, a rise in cecal butyrate levels during *A. caccae* treatment (Figure 5A) was correlated with a restoration of epithelial hypoxia (Figures 5C and 5D). By contrast, when mice with a history of Str treatment and high fat intake were treated with *E. coli* Nissle 1917 or *L. plantarum*, neither cecal butyrate levels (Figure 5A) nor epithelial hypoxia (Figures 5C and 5D) were restored. Collectively, these data supported the hypothesis that butyrate production by *A. caccae* activates epithelial PPAR-γ signaling to restore epithelial hypoxia, which in turn promotes microbiota recovery.

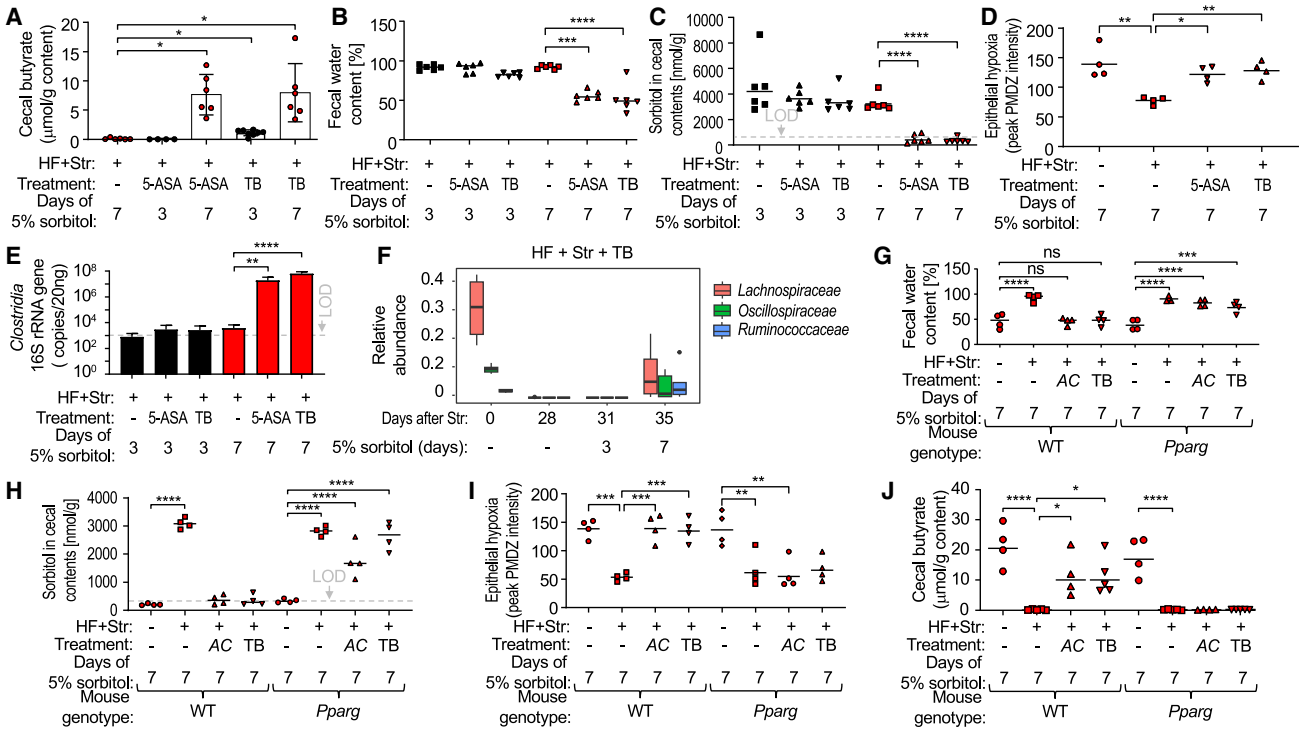

Figure 6. *A. caccae* and butyrate stimulate epithelial PPAR-γ signaling to promote microbiota recovery

Mice reared and maintained throughout the experiment on a low-fat (LF) or a high-fat (HF) diet were mock-treated or received a single dose of streptomycin (Str), respectively. 4 weeks later, mice received drinking water supplemented with 5% sorbitol and were inoculated with *A. caccae* (*AC*) or received supplementation with 5-amino salicylic acid (5-ASA) or tributyrin (TB). Samples were collected after 3 or 7 days of sorbitol supplementation.

(A–F) Experiments with C57BL/6J mice. (A) Butyrate concentrations in cecal contents. (B) Fecal water content in fecal pellets. (C) Sorbitol concentration. (D and I) Mice were injected with pimonidazole before euthanasia. Binding of pimonidazole (PMDZ) was detected using hypoxyprobe-1 primary antibody and a Cy-3 conjugated goat anti-mouse secondary antibody. (D) Average PMDZ peak intensity. (E) Absolute abundance of *Clostridia* in fecal samples was determined by real-time PCR using class-specific primers. Error bars represent standard deviation. (F) Relative abundance of *Clostridia* families containing gene sequence involved in butyrate metabolism. Box plots represent the first to third quartiles, and lines indicate median values.

(G–J) Experiments were performed with *Pparg*$^{fl/fl}$*Villin*$^{cre/-}$ mice (*Pparg*) or *Pparg*$^{fl/fl}$*Villin*$^{-/-}$ littermate controls (WT). (G) Fecal water content. (H) Sorbitol concentration. (I) Average PMDZ peak intensity. (J) Butyrate concentrations in cecal contents. *p < 0.05; **p < 0.01; ***p < 0.005; ****p < 0.001. Analysis by one-way ANOVA followed by Tukey's multiple-comparison tests (A–C, E, and G–J) or Kruskal-Wallis test (D). (C and H) LOD, limit of detection.

See also Figure S7.

To test this hypothesis, we determined whether butyrate activates epithelial PPAR-γ signaling to promote microbiota recovery in mice with prolonged sorbitol intolerance. Since butyrate is absorbed in the small intestine, we inoculated mice with tributyrin (TB), a triglyceride that is poorly absorbed in the small intestine and is cleaved by host enzymes in the large intestine to release glycerol and butyrate. Mice reared and maintained throughout the experiment on a HF diet received a single dose of Str. 4 weeks later, mice received drinking water supplemented with 5% sorbitol and were mock-treated or treated with TB. 3 days of TB treatment resulted in a small but significant increase in the cecal butyrate concentration (Figure 6A). By 7 days of TB treatment, cecal butyrate levels were markedly increased. TB treatment protected against sorbitol-induced diarrhea (Figure 6B) which was linked to depletion of sorbitol in cecal contents after 7 days of sorbitol supplementation (Figure 6C). Consistent with our hypothesis, TB restored epithelial hypoxia in the colon (Figure 6D) and enlarged the absolute *Clostridia* abundance (Figure 6E), which included a rise in the relative abundance of *Lachnospiraceae* (Figure 6F), after 7 days of treatment. These data suggested that butyrate restores hypoxia to promote microbiota recovery, a process that confers resistance to sorbitol-induced diarrhea within a week of TB supplementation.

Next, we wanted to determine whether PPAR-γ signaling in the host epithelium was required for maintaining protection against sorbitol intolerance even after *A. caccae* has been cleared. Mice lacking PPAR-γ synthesis specifically in the intestinal epithelium (*Pparg*$^{fl/fl}$*Villin*$^{cre/-}$ mice) and WT littermate controls (*Pparg*$^{fl/fl}$*Villin*$^{-/-}$ mice) reared and maintained throughout the experiment on a LF or a HF diet were mock-treated or received a single dose of Str, respectively. 4 weeks later, mice received drinking water supplemented with 5% sorbitol (Figure 4A). At the time of sorbitol exposure, mice were either mock inoculated, inoculated with *A. caccae*, or received TB treatment. Notably, in mice lacking epithelial PPAR-γ signaling, treatment with *A. caccae* or TB no longer protected against sorbitol-induced diarrhea (Figure 6G) and the accumulation of sorbitol in cecal contents (Figure 6H).

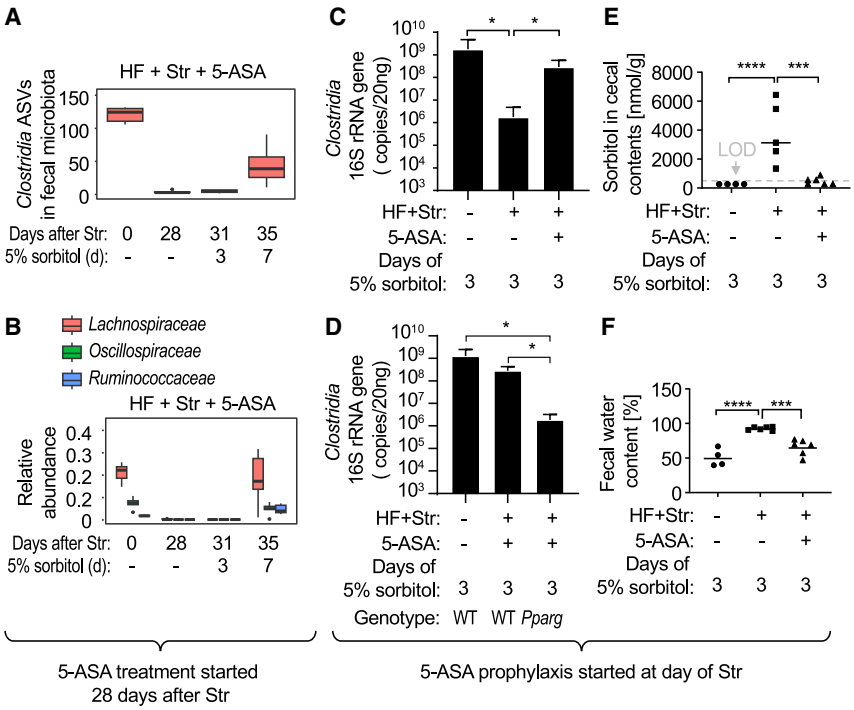

Figure 7. 5-ASA treatment prevents development of prolonged sorbitol intolerance

Mice maintained on a low-fat (LF) diet or a high-fat (HF) diet for 14 days were mock-treated or received a single dose of streptomycin (Str) by oral gavage. (A and B) 4 weeks later, mice received drinking water supplemented with 5% sorbitol and were treated by supplementing chow with 5-ASA. (A) The relative abundance of *Clostridia* in fecal samples collected from C57BL/6J mice. (B) Relative abundance of *Clostridia* families containing gene sequence involved in butyrate metabolism. Box plots represent the first to third quartiles, and lines indicate median values.

(C–F) At the time of streptomycin treatment mice were switched to chow supplemented with 5-ASA. 4 weeks later, mice received drinking water supplemented with 5% sorbitol to assess sorbitol tolerance. (C and D) Absolute abundance of *Clostridia* in fecal samples of C57BL/6J mice (C), *Pparg*$^{fl/fl}$*Villin*$^{cre/-}$ mice (*Pparg*), or *Pparg*$^{fl/fl}$*Villin*$^{-/-}$ littermate control mice (WT) (D) was determined by real-time PCR using class-specific primers. Error bars represent standard deviation. (E) Sorbitol concentration in C57BL/6J mice. LOD, limit of detection. (F) Fecal water content in samples from C57BL/6J mice. *p < 0.05; **p < 0.01; ***p < 0.005; ****p < 0.001. (C–F) Analysis by one-way ANOVA followed by Tukey's multiple-comparison tests.

Furthermore, treatment with *A. caccae* or TB no longer restored epithelial hypoxia in mice lacking epithelial PPAR-γ signaling (Figures 6I and S7). Consistent with a role of PPAR-γ signaling in promoting the recovery of butyrate-producing members of the microbiota, butyrate levels increased 1 week after treatment with *A. caccae* in littermate control mice but not in mice lacking epithelial PPAR-γ signaling (Figure 6J).

5-ASA promotes microbiota recovery to prevent sorbitol intolerance

The finding that butyrate production by *A. caccae* promoted microbiota recovery within 7 days after inoculation suggested that restoration of epithelial hypoxia could be a potential strategy for promoting microbiota recovery after antibiotic exposure. We reasoned that PPAR-γ agonists that target the host to restore epithelial hypoxia would reestablish anaerobiosis, thereby normalizing growth of obligately anaerobic *Clostridia* to prevent sorbitol intolerance. Previous work shows that the PPAR-γ agonist 5-amino salicylic acid (5-ASA)[41] restores epithelial hypoxia in mice with a history of antibiotic treatment and high fat intake.[20] We thus explored whether 5-ASA could be used for treatment or prophylaxis of sorbitol intolerance.

Mice with a history of antibiotic treatment and high fat intake (Figure 4A) received chow supplemented with 5-ASA and drinking water supplemented with 5% sorbitol. Supplementation with 5-ASA for 3 days did not alleviate signs of sorbitol intolerance. However, by 7 days of 5-ASA treatment, cecal butyrate levels were markedly increased (Figure 6A). 7 days of 5-ASA treatment protected mice against sorbitol-induced diarrhea (Figure 6B), which was linked to a depletion of sorbitol in cecal contents (Figure 6C), a restoration of epithelial hypoxia in the colon (Figure 6D), a greater absolute *Clostridia* abundance (Figure 6E), an increased richness of the *Clostridia* population (Figure 7A), and a rise in the relative abundance of *Lachnospiraceae* (Figure 7B). Collectively, these data suggested that activation of epithelial PPAR-γ signaling with 5-ASA facilitated microbiota recovery by activating epithelial PPAR-γ signaling, but this process did not restore homeostasis fast enough to provide immediate relieve from sorbitol intolerance.

To test whether 5-ASA could be used for prophylaxis, mice reared and maintained throughout the experiment on a LF or a HF diet were mock-treated or received a single dose of Str, respectively, and received prophylaxis by supplementing chow with 5-ASA starting on the day of Str treatment. 4 weeks later, mice received drinking water supplemented with 5% sorbitol to assess sorbitol tolerance. Prophylaxis with 5-ASA restored a normal absolute abundance of *Clostridia* in Str-treated mice on a HF diet (Figure 7C). 5-ASA drove this change in the microbiota composition by activating PPAR-γ in the intestinal epithelium, because 5-ASA prophylaxis no longer increased *Clostridia* levels in mice lacking PPAR-γ synthesis specifically in the intestinal epithelium (*Pparg*$^{fl/fl}$*Villin*$^{cre/-}$ mice) (Figure 7D). 5-ASA prophylaxis prevented accumulation of sorbitol in cecal contents during sorbitol supplementation (Figure 7E) and reduced fecal water content (Figure 7F). Thus, prophylactic activation of epithelial PPAR-γ signaling with 5-ASA prevented development of prolonged sorbitol intolerance after exposure to antibiotics and high fat intake by promoting microbiota recovery, thereby normalizing microbial sorbitol catabolism.

DISCUSSION

Up to 30% of the population in high-income countries experience episodes of carbohydrate intolerance, with abdominal complaints being associated most commonly with lactose, fructose, or sorbitol.[42] Lactose and fructose intolerance can be explained by malabsorption in the ileum due to congenital or acquired defects in specific host enzymes or transport systems.[43] Sorbitol intolerance is commonly included in the category of carbohydrate malabsorption.[42] However, since humans lack a specific sorbitol transporter, its uptake relies on passive diffusion, resulting in poor absorption in the small intestine even in healthy individuals. There is no experimental evidence to suggest that patients with sorbitol intolerance exhibit reduced uptake of sorbitol by passive diffusion.[44] Instead, our results suggest that in healthy individuals, microbial sorbitol catabolism protects against symptoms of sorbitol intolerance arising from an inherently poor absorption of this polyol. Here we show that sorbitol intolerance arises from an impairment of microbial sorbitol catabolism, a finding with implications for diagnosis, pathophysiology, treatment, and prevention.

The development of carbohydrate intolerance tests that reliably predict the outcome of dietary management remains a clinical challenge in the field of functional bowel disease.[43] Here we show that measurements of microbiota-derived SDH levels in the feces and the abundance of SDH gene sequences in the metagenome predict sorbitol intolerance in a mouse model. Furthermore, the analysis of human fecal samples suggested that low SDH levels correlate with patients exhibiting intolerance to sugar-free food. Thus, it may be possible to develop microbiota-based diagnostic tests for sorbitol intolerance in high-risk groups, which represents a promising area for future research.

By developing an animal model for prolonged sorbitol intolerance, our results provide insights into the pathophysiology of this condition. The observation that exposure to antibiotics in combination with high fat intake impairs microbial sorbitol catabolism by lowering the abundance of *Clostridia* challenges conventional wisdom that prolonged sorbitol intolerance is caused by malabsorption.[12,42] Exposure to antibiotics and high fat intake are also environmental risk factors involved in the pathophysiology of IBD.[45–50] Epidemiological studies from Western countries, where these risk factors are more prevalent, report a higher incidence of carbohydrate intolerance compared with Asian countries,[42] and feces of East Asian subjects exhibit increased levels of short-chain fatty acids and greater abundance of reads encoding short-chain fatty acid-related metabolic pathways binned to *Clostridia* compared with white subjects.[51] A reduced relative abundance of *Clostridia* in IBD patients is well documented.[52–55] Our results show that a combination of environmental risk factors can give rise to prolonged sorbitol intolerance, which is observed in some patients with quiescent IBD.[8,9] Clinical trials show a correlation between carbohydrate intake (including polyols) and gastrointestinal symptoms in IBD patients.[11,56,57] These clinical observations align well with our finding that diminished butyrate production and a reduced abundance of *Clostridia* in the fecal microbiota are functionally linked to prolonged sorbitol intolerance in a mouse model.

Epithelial hypoxia limits the diffusion of oxygen into the intestinal lumen to maintain anaerobiosis,[58] thereby providing a host environment that favors growth of obligately anaerobic bacteria, such as *Clostridia*.[59] Antibiotic-mediated disruption of the colonic microbiota depletes short-chain fatty acids, which in turn triggers a shift in epithelial metabolism to increase the availability of host-derived oxygen.[40] A HF diet rich in saturated fatty acids triggers oxidative stress in host cells[60] by inducing elevated mitochondrial hydrogen peroxide production.[61,62] Through this mechanism, a prolonged HF diet impairs recovery of mitochondrial bioenergetics after antibiotic treatment, thereby interfering with microbiota recovery.[20] Since increased epithelial oxygenation is ultimately responsible for an impaired microbiota recovery after antibiotic exposure, it should be possible to prevent the development of prolonged sorbitol intolerance after exposure to antibiotics and high fat intake by restoring host functions that maintain the colonic epithelium in a state of physiological hypoxia. Our results suggest that prophylaxis with 5-ASA, a drug that activates epithelial PPAR-γ signaling to stimulate mitochondrial activity,[63] can reestablish epithelial hypoxia and promote microbiota recovery after antibiotic treatment even in the face of high fat intake. These data identify the intestinal epithelium as a potential treatment target to prevent the development of prolonged sorbitol intolerance.

The finding that prolonged sorbitol intolerance is due to impaired microbial sorbitol catabolism suggests that the microbiota represents a second potential treatment target. One treatment option might be the use of sorbitol-consuming probiotics, such as *E. coli* Nissle 1917 or *L. plantarum*, to augment microbial sorbitol catabolism in patients with sorbitol intolerance. However, the protective effect of probiotics was dependent on reaching high numbers in the feces. Such high colonization levels might be difficult to accomplish with some probiotics. Furthermore, high colonization levels of *E. coli* Nissle 1917 might not be desirable, since intestinal domination by *Enterobacterales* is considered a microbial signature of dysbiosis.[28,64] Interestingly, our data identify *A. caccae* as a second-generation probiotic that targets both the host and the microbes to protect against sorbitol intolerance. The ability of *A. caccae* to catabolize sorbitol resulted in a depletion of this polyol from cecal contents when the probiotic was abundant, which conferred protection against transient sorbitol intolerance after antibiotic exposure. Importantly, *A. caccae* still conferred protection against prolonged sorbitol intolerance even when the abundance of the probiotic was low, which was linked to its ability to produce butyrate. Butyrate stimulates PPAR-γ signaling in the host to restore epithelial hypoxia,[40] which promoted microbiota recovery within a week after inoculating mice with *A. caccae*. Once microbiota recovery was complete, a high abundance of *A. caccae* was no longer required to confer protection against sorbitol intolerance. Thus, the appeal of using this second-generation probiotic is that the sorbitol catabolism of *A. caccae* provides immediate relief from sorbitol intolerance, whereas its ability to produce butyrate promotes microbiota recovery within a week, thereby allowing other bacteria that metabolize sorbitol to grow to numbers that are high enough to deplete this polyol.

Limitations of the study

Antibiotic-naive mice tolerate supplementation with up to 5% sorbitol, which is equivalent to a daily intake of 20–30 g in humans, a dosage that can induce symptoms of carbohydrate intolerance in healthy volunteers.[5] A possible reason why mice can tolerate a higher sorbitol intake than humans is that these hindgut fermenters possess an enlarged cecum to slow digesta flow, which aids carbohydrate catabolism by the microbiota.[65] These morphological and functional differences between the gastrointestinal tracts of mice and humans represent a limitation of rodent models. Therefore, clinical studies will be needed to further test the hypothesis that probiotics or PPAR-γ agonists can be used to treat or prevent sorbitol intolerance.

STAR★METHODS

Detailed methods are provided in the online version of this paper and include the following:

- KEY RESOURCES TABLE
- RESOURCE AVAILABILITY
  - Lead contact
  - Materials availability
  - Data and code availability
- EXPERIMENTAL MODEL AND STUDY PARTICIPANT DETAILS
  - Mouse Models
  - Bacterial strains and culture conditions
  - Human studies
- METHOD DETAILS
  - Construction of E. coli Nissle 1917 ΔsrlAEB
  - 16S rRNA gene amplicon sequencing sample preparation, library preparation, and Sequencing
  - 16S rRNA gene amplicon sequencing analysis
  - Shotgun Metagenome Data Analysis
  - D-Sorbitol Measurements
  - Sorbitol Dehydrogenase Activity Measurements
  - Fecal water content
  - Determining bacterial absolute abundance using quantitative real-time PCR
  - *In vitro* measurement of sorbitol in E. coli culture supernatants
  - *In vitro* growth assay of Clostridia strains
  - Hypoxia staining and imaging
  - Butyrate analysis
- QUANTIFICATION AND STATISTICAL ANALYSIS
  - Microbiota profiling and metagenomic analysis
- ADDITIONAL RESOURCES
  - Description: URL

ACKNOWLEDGMENTS

We would like to thank K. Honda for kindly providing 17 human fecal isolates of butyrate producers belonging to the classes *Clostridia* and *Erysipelotrichia*. We would like to thank Ardeypharm GmbH for kindly providing *E. coli* strain Nissle 1917. This work was supported by the Kenneth Rainin Foundation award #20230029 (A.J.B. and J.-Y.L.) and the 2020 Tri-Institutional Partnership in Microbiome Research Initiative with funding from the University of California, San Francisco, University of California, Davis, and the National Microbiome Data Collaborative (NMDC, award 000583). The work conducted by the National Microbiome Data Collaborative (https://ror.org/05cwx3318) is supported by the Genomic Science Program in the U.S. Department of Energy, Office of Science, Office of Biological and Environmental Research (BER) under contract numbers DE-AC02-05CH11231 (LBNL), 89233218CNA000001 (LANL), and DE-AC05-76RL01830 (PNNL). Sequencing library preparations and sequencing were carried out at the DNA Technologies and Expression Analysis Cores at the UC Davis Genome Center, supported by NIH Shared Instrumentation Grant 1S10OD010786-01. E.T.S. was supported by the National Science Foundation grant #1650042. Work in A.J.B.'s laboratory was supported by Crohn's and Colitis Foundation of America award 650976 and by Public Health Service grants AI044170, AI096528, AI112445, AI112949, AI146432, and AI153069. P.J.T. was supported by the National Institutes of Health (2R01HL122593, 1R01AT011117, 1R01DK114034, and 1R01AR074500), was a Chan Zuckerberg Biohub-San Francisco Investigator, and held an Investigators in the Pathogenesis of Infectious Disease Award from the Burroughs Wellcome Fund.

AUTHOR CONTRIBUTIONS

J.-Y.L. provided study design, supervised personnel, performed mouse experiments, and analyzed the data. C.R.T. analyzed the metagenomic analysis data and microbiota profiling data. S.P.M. helped perform mouse experiments. M.K. and E.A.E.-F. performed assembly, annotation, and binning of metagenomic data. A.W.L.R. generated gene-deletion mutant bacteria for mouse experiments. H.N. and K.Y. helped perform mouse experiments. H.L.P.M. performed measurements of butyrate concentrations. E.T.S. helped perform mouse experiments and validation of the manuscript. M.L.M. contributed to the design of the experiments. P.J.T. contributed to the design of the experiments and validation of the manuscript. A.J.B. was a major contributor in conceptualization, supervision, and writing the manuscript.

DECLARATION OF INTERESTS

The authors declare no competing interests.

Received: October 25, 2022
Revised: September 27, 2023
Accepted: January 18, 2024
Published: February 15, 2024

REFERENCES

1. Lenhart, A., and Chey, W.D. (2017). A Systematic Review of the Effects of Polyols on Gastrointestinal Health and Irritable Bowel Syndrome. Adv. Nutr. *8*, 587–596.
2. Tennant, D.R. (2014). Potential intakes of total polyols based on UK usage survey data. Food Addit. Contam.: A *34*, 574–586.
3. Wallaart, R.A.M. (1980). .1Distribution of Sorbitol in Rosaceae. Phytochemistry *19*, 2603–2610.
4. Reele, S.B., and Chodos, D.J. (1985). Sorbitol induced diarrheal illness model. Int. J. Clin. Pharmacol. Ther. Toxicol. *23*, 403–405.
5. Corazza, G.R., Strocchi, A., Rossi, R., Sirola, D., and Gasbarrini, G. (1988). Sorbitol malabsorption in normal volunteers and in patients with coeliac disease. Gut *29*, 44–48.
6. Magge, S., and Lembo, A. (2012). Low-FODMAP Diet for Treatment of Irritable Bowel Syndrome. Gastroenterol. Hepatol. (N Y) *8*, 739–745.
7. de Roest, R.H., Dobbs, B.R., Chapman, B.A., Batman, B., O'Brien, L.A., Leeper, J.A., Hebblethwaite, C.R., and Gearry, R.B. (2013). The low FODMAP diet improves gastrointestinal symptoms in patients with irritable bowel syndrome: a prospective study. Int. J. Clin. Pract. *67*, 895–903.
8. Gearry, R.B., Irving, P.M., Barrett, J.S., Nathan, D.M., Shepherd, S.J., and Gibson, P.R. (2009). Reduction of dietary poorly absorbed short-chain carbohydrates (FODMAPs) improves abdominal symptoms in

patients with inflammatory bowel disease-a pilot study. J. Crohns Colitis *3*, 8–14.

9. Gibson, P.R. (2017). Use of the low-FODMAP diet in inflammatory bowel disease. J. Gastroenterol. Hepatol. *32*, 40–42.
10. Rumessen, J.J., and Gudmand-Høyer, E. (1988). Functional bowel disease: malabsorption and abdominal distress after ingestion of fructose, sorbitol, and fructose-sorbitol mixtures. Gastroenterology *95*, 694–700.
11. Cox, S.R., Prince, A.C., Myers, C.E., Irving, P.M., Lindsay, J.O., Lomer, M.C., and Whelan, K. (2017). Fermentable Carbohydrates [FODMAPs] Exacerbate Functional Gastrointestinal Symptoms in Patients With Inflammatory Bowel Disease: A Randomised, Double-blind, Placebo-controlled, Cross-over, Re-challenge Trial. J. Crohns Colitis *11*, 1420–1429.
12. Hammer, H.F., and Hammer, J. (2012). Diarrhea caused by carbohydrate malabsorption. Gastroenterol. Clin. North Am. *41*, 611–627.
13. Rao, S.S., Edwards, C.A., Austen, C.J., Bruce, C., and Read, N.W. (1988). Impaired colonic fermentation of carbohydrate after ampicillin. Gastroenterology *94*, 928–932.
14. Hattori, K., Akiyama, M., Seki, N., Yakabe, K., Hase, K., and Kim, Y.G. (2021). Gut Microbiota Prevents Sugar Alcohol-Induced Diarrhea. Nutrients *13*, 2029.
15. Stecher, B., Robbiani, R., Walker, A.W., Westendorf, A.M., Barthel, M., Kremer, M., Chaffron, S., Macpherson, A.J., Buer, J., Parkhill, J., et al. (2007). Salmonella enterica serovar typhimurium exploits inflammation to compete with the intestinal microbiota. PLoS Biol. *5*, 2177–2189.
16. Rivera-Chávez, F., Zhang, L.F., Faber, F., Lopez, C.A., Byndloss, M.X., Olsan, E.E., Xu, G., Velazquez, E.M., Lebrilla, C.B., Winter, S.E., and Baumler, A.J. (2016). Depletion of Butyrate-Producing Clostridia from the Gut Microbiota Drives an Aerobic Luminal Expansion of Salmonella. Cell Host Microbe *19*, 443–454.
17. Gillis, C.C., Hughes, E.R., Spiga, L., Winter, M.G., Zhu, W., Furtado de Carvalho, T., Chanin, R.B., Behrendt, C.L., Hooper, L.V., Santos, R.L., and Winter, S.E. (2018). Dysbiosis-Associated Change in Host Metabolism Generates Lactate to Support Salmonella Growth. Cell Host Microbe *23*, 54–64.e6.
18. Chassany, O., Michaux, A., and Bergmann, J.F. (2000). Drug-induced diarrhoea. Drug Saf. *22*, 53–72.
19. Fernandez, K., D'Souza, S., Ahn, J.J., Singh, S., Bacasen, E.M., Mashiach, D., Mishail, D., Kao, T., Thai, J., Hwang, S., et al. (2020). Mutations induced by Bleomycin, 4-nitroquinoline-1-oxide, and hydrogen peroxide in the rpoB gene of Escherichia coli: Perspective on Mutational Hotspots. Mutat. Res. *821*, 111702.
20. Lee, J.Y., Cevallos, S.A., Byndloss, M.X., Tiffany, C.R., Olsan, E.E., Butler, B.P., Young, B.M., Rogers, A.W.L., Nguyen, H., Kim, K., et al. (2020). High-Fat Diet and Antibiotics Cooperatively Impair Mitochondrial Bioenergetics to Trigger Dysbiosis that Exacerbates Pre-inflammatory Bowel Disease. Cell Host Microbe *28*, 273–284.e6.
21. D'haens, G., Ferrante, M., Vermeire, S., Baert, F., Noman, M., Moortgat, L., Geens, P., Iwens, D., Aerden, I., Van Assche, G., et al. (2012). Fecal calprotectin is a surrogate marker for endoscopic lesions in inflammatory bowel disease. Inflamm. Bowel Dis. *18*, 2218–2224.
22. Spiller, R., and Major, G. (2016). IBS and IBD - separate entities or on a spectrum? Nat. Rev. Gastroenterol. Hepatol. *13*, 613–621.
23. Spiller, R., and Lam, C. (2011). The shifting interface between IBS and IBD. Curr. Opin. Pharmacol. *11*, 586–592.
24. Colombel, J.F., Shin, A., and Gibson, P.R. (2019). AGA Clinical Practice Update on Functional Gastrointestinal Symptoms in Patients With Inflammatory Bowel Disease: Expert Review. Clin. Gastroenterol. Hepatol. *17*, 380–390.e1.
25. Adeolu, M., Alnajar, S., Naushad, S., and S Gupta, R. (2016). Genome-based phylogeny and taxonomy of the 'Enterobacteriales': proposal for Enterobacterales ord. nov. divided into the families Enterobacteriaceae, Erwiniaceae fam. nov., Pectobacteriaceae fam. nov., Yersiniaceae fam. nov., Hafniaceae fam. nov., Morganellaceae fam. nov., and Budviciaceae fam. nov. Int. J. Syst. Evol. Microbiol. *66*, 5575–5599.
26. Rigottier-Gois, L. (2013). Dysbiosis in inflammatory bowel diseases: the oxygen hypothesis. ISME J. *7*, 1256–1261.
27. Rizzatti, G., Lopetuso, L.R., Gibiino, G., Binda, C., and Gasbarrini, A. (2017). Proteobacteria: A Common Factor in Human Diseases. BioMed Res. Int. *2017*, 9351507.
28. Shin, N.R., Whon, T.W., and Bae, J.W. (2015). Proteobacteria: microbial signature of dysbiosis in gut microbiota. Trends Biotechnol. *33*, 496–503.
29. Kanehisa, M., and Goto, S. (2000). KEGG: kyoto encyclopedia of genes and genomes. Nucleic Acids Res. *28*, 27–30.
30. Sola-Carvajal, A., García-García, M.I., García-Carmona, F., and Sánchez-Ferrer, Á. (2012). Insights into the evolution of sorbitol metabolism: phylogenetic analysis of SDR196C family. BMC Evol. Biol. *12*, 147.
31. Soemphol, W., Saichana, N., Yakushi, T., Adachi, O., Matsushita, K., and Toyama, H. (2012). Characterization of Genes Involved in D-Sorbitol Oxidation in Thermotolerant Gluconobacter frateurii. Biosci. Biotechnol. Biochem. *76*, 1497–1505.
32. Riveros-Rosas, H., Julián-Sánchez, A., Villalobos-Molina, R., Pardo, J.P., and Piña, E. (2003). Diversity, taxonomy and evolution of medium-chain dehydrogenase/reductase superfamily. Eur. J. Biochem. *270*, 3309–3334.
33. Nissle, A. (1925). Weiteres über grundlagen und praxis der mutaflorbehandlung. DMW Dtsch. Med. Wochenschr. *51*, 1809–1813.
34. Tiffany, C.R., Lee, J.Y., Rogers, A.W.L., Olsan, E.E., Morales, P., Faber, F., and Bäumler, A.J. (2021). The metabolic footprint of Clostridia and Erysipelotrichia reveals their role in depleting sugar alcohols in the cecum. Microbiome *9*, 174.
35. O'Toole, P.W., Marchesi, J.R., and Hill, C. (2017). Next-generation probiotics: the spectrum from probiotics to live biotherapeutics. Nat. Microbiol. *2*, 17057.
36. Narushima, S., Sugiura, Y., Oshima, K., Atarashi, K., Hattori, M., Suematsu, M., and Honda, K. (2014). Characterization of the 17 strains of regulatory T cell-inducing human-derived Clostridia. Gut Microbes *5*, 333–339.
37. Walker, A.W., Ince, J., Duncan, S.H., Webster, L.M., Holtrop, G., Ze, X., Brown, D., Stares, M.D., Scott, P., Bergerat, A., et al. (2011). Dominant and diet-responsive groups of bacteria within the human colonic microbiota. ISME J. *5*, 220–230.
38. Arumugam, M., Raes, J., Pelletier, E., Le Paslier, D., Yamada, T., Mende, D.R., Fernandes, G.R., Tap, J., Bruls, T., Batto, J.M., et al. (2011). Enterotypes of the human gut microbiome. Nature *473*, 174–180.
39. Vital, M., Howe, A.C., and Tiedje, J.M. (2014). Revealing the bacterial butyrate synthesis pathways by analyzing (meta)genomic data. mBio *5*, e00889.
40. Byndloss, M.X., Olsan, E.E., Rivera-Chávez, F., Tiffany, C.R., Cevallos, S.A., Lokken, K.L., Torres, T.P., Byndloss, A.J., Faber, F., Gao, Y., et al. (2017). Microbiota-activated PPAR-g signaling inhibits dysbiotic Enterobacteriaceae expansion. Science *357*, 570–575.
41. Rousseaux, C., Lefebvre, B., Dubuquoy, L., Lefebvre, P., Romano, O., Auwerx, J., Metzger, D., Wahli, W., Desvergne, B., Naccari, G.C., et al. (2005). Intestinal antiinflammatory effect of 5-aminosalicylic acid is dependent on peroxisome proliferator-activated receptor-gamma. J. Exp. Med. *201*, 1205–1215.
42. Born, P. (2007). Carbohydrate malabsorption in patients with non-specific abdominal complaints. World J. Gastroenterol. *13*, 5687–5691.
43. Fernández-Bañares, F. (2022). Carbohydrate Maldigestion and Intolerance. Nutrients *14*, 1923.
44. Fernandez-Bañares, F., Esteve-Pardo, M., Humbert, P., de Leon, R., Llovet, J.M., and Gassull, M.A. (1991). Role of fructose-sorbitol

malabsorption in the irritable bowel syndrome. Gastroenterology *101*, 1453–1454.

45. Albenberg, L.G., Lewis, J.D., and Wu, G.D. (2012). Food and the gut microbiota in inflammatory bowel diseases: a critical connection. Curr. Opin. Gastroenterol. *28*, 314–320.
46. Frolkis, A., Dieleman, L.A., Barkema, H.W., Panaccione, R., Ghosh, S., Fedorak, R.N., Madsen, K., and Kaplan, G.G.; Alberta IBD Consortium (2013). Environment and the inflammatory bowel diseases. Can. J. Gastroenterol. *27*, e18–e24.
47. Hildebrand, H., Malmborg, P., Askling, J., Ekbom, A., and Montgomery, S.M. (2008). Early-life exposures associated with antibiotic use and risk of subsequent Crohn's disease. Scand. J. Gastroenterol. *43*, 961–966.
48. Hviid, A., Svanström, H., and Frisch, M. (2011). Antibiotic use and inflammatory bowel diseases in childhood. Gut *60*, 49–54.
49. Lewis, J.D. (2014). A review of the epidemiology of inflammatory bowel disease with a focus on diet, infections and antibiotic exposure. Nestle Nutr. Inst. Workshop Ser. *79*, 1–18.
50. Zou, Y., Wu, L., Xu, W., Zhou, X., Ye, K., Xiong, H., Song, C., and Xie, Y. (2020). Correlation between antibiotic use in childhood and subsequent inflammatory bowel disease: a systematic review and meta-analysis. Scand. J. Gastroenterol. *55*, 301–311.
51. Ang, Q.Y., Alba, D.L., Upadhyay, V., Bisanz, J.E., Cai, J., Lee, H.L., Barajas, E., Wei, G., Noecker, C., Patterson, A.D., et al. (2021). The East Asian gut microbiome is distinct from colocalized White subjects and connected to metabolic health. eLife *10*, e70349.
52. Alam, M.T., Amos, G.C.A., Murphy, A.R.J., Murch, S., Wellington, E.M.H., and Arasaradnam, R.P. (2020). Microbial imbalance in inflammatory bowel disease patients at different taxonomic levels. Gut Pathog. *12*, 1.
53. Lepage, P., Häsler, R., Spehlmann, M.E., Rehman, A., Zvirbliene, A., Begun, A., Ott, S., Kupcinskas, L., Doré, J., Raedler, A., and Schreiber, S. (2011). Twin study indicates loss of interaction between microbiota and mucosa of patients with ulcerative colitis. Gastroenterology *141*, 227–236.
54. Machiels, K., Joossens, M., Sabino, J., De Preter, V., Arijs, I., Eeckhaut, V., Ballet, V., Claes, K., Van Immerseel, F., Verbeke, K., et al. (2014). A decrease of the butyrate-producing species Roseburia hominis and Faecalibacterium prausnitzii defines dysbiosis in patients with ulcerative colitis. Gut *63*, 1275–1283.
55. Sartor, R.B. (2008). Microbial influences in inflammatory bowel diseases. Gastroenterology *134*, 577–594.
56. Zhan, Y.L., Zhan, Y.A., and Dai, S.X. (2018). Is a low FODMAP diet beneficial for patients with inflammatory bowel disease? A meta-analysis and systematic review. Clin. Nutr. *37*, 123–129.
57. Bodini, G., Zanella, C., Crespi, M., Lo Pumo, S., Demarzo, M.G., Savarino, E., Savarino, V., and Giannini, E.G. (2019). A randomized, 6-wk trial of a low FODMAP diet in patients with inflammatory bowel disease. Nutrition *67–68*, 110542.
58. Litvak, Y., Byndloss, M.X., and Bäumler, A.J. (2018). Colonocyte metabolism shapes the gut microbiota. Science *362*, eaat9076.
59. Miller, B.M., Liou, M.J., Lee, J.Y., and Bäumler, A.J. (2021). The longitudinal and cross-sectional heterogeneity of the intestinal microbiota. Curr. Opin. Microbiol. *63*, 221–230.
60. Gulhane, M., Murray, L., Lourie, R., Tong, H., Sheng, Y.H., Wang, R., Kang, A., Schreiber, V., Wong, K.Y., Magor, G., et al. (2016). High Fat Diets Induce Colonic Epithelial Cell Stress and Inflammation that is Reversed by IL-22. Sci. Rep. *6*, 28990.
61. Cardoso, A.R., Kakimoto, P.A., and Kowaltowski, A.J. (2013). Diet-sensitive sources of reactive oxygen species in liver mitochondria: role of very long chain acyl-CoA dehydrogenases. PLoS One *8*, e77088.
62. Kakimoto, P.A., Tamaki, F.K., Cardoso, A.R., Marana, S.R., and Kowaltowski, A.J. (2015). H2O2 release from the very long chain acyl-CoA dehydrogenase. Redox Biol. *4*, 375–380.
63. Cevallos, S.A., Lee, J.Y., Velazquez, E.M., Foegeding, N.J., Shelton, C.D., Tiffany, C.R., Parry, B.H., Stull-Lane, A.R., Olsan, E.E., Savage, H.P., et al. (2021). 5-Aminosalicylic Acid Ameliorates Colitis and Checks Dysbiotic Escherichia coli Expansion by Activating PPAR-gamma Signaling in the Intestinal Epithelium. mBio *12*. e03227–e03220.
64. Litvak, Y., Byndloss, M.X., Tsolis, R.M., and Bäumler, A.J. (2017). Dysbiotic Proteobacteria expansion: a microbial signature of epithelial dysfunction. Curr. Opin. Microbiol. *39*, 1–6.
65. Karasov, W.H., and Douglas, A.E. (2013). Comparative digestive physiology. Compr. Physiol. *3*, 741–783.
66. Pal, D., Venkova-Canova, T., Srivastava, P., and Chattoraj, D.K. (2005). Multipartite regulation of rctB, the replication initiator gene of Vibrio cholerae chromosome II. J. Bacteriol. *187*, 7167–7175.
67. Simon, R., Priefer, U., and Pühler, A. (1983). A Broad Host Range Mobilization System for In Vivo Genetic Engineering: Transposon Mutagenesis in Gram Negative Bacteria. Bio/Technology *1*, 784–791.
68. Tachon, S., Lee, B., and Marco, M.L. (2014). Diet alters probiotic Lactobacillus persistence and function in the intestine. Environ. Microbiol. *16*, 2915–2926.
69. Atarashi, K., Tanoue, T., Oshima, K., Suda, W., Nagano, Y., Nishikawa, H., Fukuda, S., Saito, T., Narushima, S., Hase, K., et al. (2013). Treg induction by a rationally selected mixture of Clostridia strains from the human microbiota. Nature *500*, 232–236.
70. Atarashi, K., Tanoue, T., Shima, T., Imaoka, A., Kuwahara, T., Momose, Y., Cheng, G., Yamasaki, S., Saito, T., Ohba, Y., et al. (2011). Induction of colonic regulatory T cells by indigenous Clostridium species. Science *331*, 337–341.
71. Edwards, R.A., Keller, L.H., and Schifferli, D.M. (1998). Improved allelic exchange vectors and their use to analyze 987P fimbria gene expression. Gene *207*, 149–157.
72. Lopez, C.A., Winter, S.E., Rivera-Chávez, F., Xavier, M.N., Poon, V., Nuccio, S.P., Tsolis, R.M., and Bäumler, A.J. (2012). Phage-mediated acquisition of a type III secreted effector protein boosts growth of salmonella by nitrate respiration. mBio *3*. e00143–e00112.
73. Spees, A.M., Wangdi, T., Lopez, C.A., Kingsbury, D.D., Xavier, M.N., Winter, S.E., Tsolis, R.M., and Bäumler, A.J. (2013). Streptomycin-induced inflammation enhances Escherichia coli gut colonization through nitrate respiration. mBio *4*. e00935–e00919.
74. Wang, R.F., and Kushner, S.R. (1991). Construction of versatile low-copy-number vectors for cloning, sequencing and gene expression in Escherichia coli. Gene *100*, 195–199.
75. Croswell, A., Amir, E., Teggatz, P., Barman, M., and Salzman, N.H. (2009). Prolonged impact of antibiotics on intestinal microbial ecology and susceptibility to enteric Salmonella infection. Infect. Immun. *77*, 2741–2753.
76. Resendiz-Nava, C.N., Silva-Rojas, H.V., Rebollar-Alviter, A., Rivera-Pastrana, D.M., Mercado-Silva, E.M., and Nava, G.M. (2021). A Comprehensive Evaluation of Enterobacteriaceae Primer Sets for Analysis of Host-Associated Microbiota. Pathogens *11*, 17.
77. Kuczynski, J., Stombaugh, J., Walters, W.A., González, A., Caporaso, J.G., and Knight, R. (2012). Using QIIME to analyze 16S rRNA gene sequences from microbial communities. Curr. Protoc. Microbiol. *Chapter 1*. Unit 1E.5.
78. Bolger, A.M., Lohse, M., and Usadel, B. (2014). Trimmomatic: a flexible trimmer for Illumina sequence data. Bioinformatics *30*, 2114–2120.
79. Callahan, B.J., McMurdie, P.J., Rosen, M.J., Han, A.W., Johnson, A.J., and Holmes, S.P. (2016). DADA2: High-resolution sample inference from Illumina amplicon data. Nat. Methods *13*, 581–583.
80. McMurdie, P.J., and Holmes, S. (2013). phyloseq: an R package for reproducible interactive analysis and graphics of microbiome census data. PLoS One *8*, e61217.
81. Love, M.I., Huber, W., and Anders, S. (2014). Moderated estimation of fold change and dispersion for RNA-seq data with DESeq2. Genome Biol. *15*, 550.

82. Segata, N., Izard, J., Waldron, L., Gevers, D., Miropolsky, L., Garrett, W.S., and Huttenhower, C. (2011). Metagenomic biomarker discovery and explanation. Genome Biol. *12*, R60.

83. Sievers, F., and Higgins, D.G. (2014). Clustal omega. Curr. Protoc. Bioinformatics *48*, 3.13.1–3.13.16. 3 13 11.

84. Hugerth, L.W., Wefer, H.A., Lundin, S., Jakobsson, H.E., Lindberg, M., Rodin, S., Engstrand, L., and Andersson, A.F. (2014). DegePrime, a program for degenerate primer design for broad-taxonomic-range PCR in microbial ecology studies. Appl. Environ. Microbiol. *80*, 5116–5123.

85. Nurk, S., Meleshko, D., Korobeynikov, A., and Pevzner, P.A. (2017). metaSPAdes: a new versatile metagenomic assembler. Genome Res. *27*, 824–834.

86. Tiffany, C.R., and Bäumler, A.J. (2019). omu, a Metabolomics Count Data Analysis Tool for Intuitive Figures and Convenient Metadata Collection. Microbiol. Resour. Announc. *8*. e00129–e00119.

87. Clum, A., Huntemann, M., Bushnell, B., Foster, B., Foster, B., Roux, S., Hajek, P.P., Varghese, N., Mukherjee, S., Reddy, T.B.K., et al. (2021). DOE JGI Metagenome Workflow. mSystems *6*. https://doi.org/10.1128/mSystems.00804-20.

88. Theriot, C.M., Koenigsknecht, M.J., Carlson, P.E., Hatton, G.E., Nelson, A.M., Li, B., Huffnagle, G.B., Z Li, J., and Young, V.B. (2014). Antibiotic-induced shifts in the mouse gut microbiome and metabolome increase susceptibility to Clostridium difficile infection. Nat. Commun. *5*, 3114.

STAR★METHODS

KEY RESOURCES TABLE

REAGENT or RESOURCE	SOURCE	IDENTIFIER
Bacterial and virus strains		
E. coli Nissle 1917 (O6:K5:H1)	Nissle[33]	*E. coli* Nissle 1917
E. coli Nissle *ΔslrAEB*	This study	*slrAEB* mutant
E. coli DH5α–1 λ*pir*	Pal et al.[66]	DH5α–1 λ*pir*
E. coli S17–1 λ*pir*	Simon et al.[67]	S17–1 λ*pir*
E. coli TOP10	Invitrogen	*E. coli* TOP10
Lactiplantibacillus plantarum NCIMB8826-R	Tachon et al.[68]	NCIMB8826-R
Anaerostipes caccae	Tiffany et al.[34]; Atarashi et al.[69,70]	N/A
Enterocloster aspargiforme	Tiffany et al.[34]; Atarashi et al.[69,70]	N/A
Biological samples		
Human fecal samples	Lee et al.[20]	N/A
Recombinant DNA		
Addgene plasmid #43828	Edwards et al.[71]	pRE112
Flanking regions of the *srlAEB* operon cloned in plasmid pRE112	This study	pAWLR80
Ori(R101) repA101tsCarb^r	Lopez et al.[72]	pSW172
pWSK29::Ω cassette	Spees et al.[73]	pCAL61
Cloning vector pWSK29	Wang and Kushner[74]	pWSK29
srlAEB operon cloned into pWSK29	This study	pAWLR169
Chemicals, peptides, and recombinant proteins		
D-sorbitol	Sigma Aldrich	Cat#: 240850
Streptomycin sulfate	Fluka	Cat#: 85884
5-aminosalicylic acid	Sigma Aldrich	Cat#: A3537
Tributyrin	Sigma Aldrich	Cat#: W222322
DAPI	Sigma Aldrich	Cat#: D9542
Critical commercial assays		
SYBR green PCR master mix	Life Technologies	Cat#: 4309155
D-sorbitol colorimetric assay kit	Biovision	Cat#: K631
Sorbitol Dehydrogenase assay kit (colorimetric)	LSBio	Cat#: LS-K239
DNeasy PowerSoil Pro Kits	QIAGEN	Cat#: 47016
NEBuilder® HiFi DNA Assembly Master Mix	New England Biolabs	Cat#: E2621
QIAprep Spin Miniprep Kit	New England Biolabs	Cat#: 27106
Q5 Hot Start 2x Master Mix	New England Biolabs	Cat#: M0494S
QIAquick PCR Purification Kit	QIAGEN	Cat#: 28104
MyTaq™ Red Mix	Meridian Bioscience	Cat#: BIO-25043
KAPA2G Robust HotStart PCR Kit	Roche	Cat#: 07961057001
Qubit™ dsDNA HS and BR Assay Kits	Invitrogen	Cat#: Q32850
Ampure XP	Beckman Coulter	Cat#: A63882
DNA clean-up kit	Zymo Research	Cat#: D4017
TOPO™ TA Cloning kit	Invitrogen	Cat#: K455001
EcoRI-HF	New England Biolabs	Cat#: R3101
SacI-HF	New England Biolabs	Cat#: R3156
BamHI	New England Biolabs	Cat#:R1036
Gibson Assembly Master Mix	New England Biolabs	Cat#: E2611

(*Continued on next page*)

Continued

REAGENT or RESOURCE	SOURCE	IDENTIFIER
Antibodies		
Mouse anti-pimonidazole monoclonal antibody MAb1	Hydroxyprobe	Hypoxyprobe™-1 Kit, HP1-1000; lot 06242014
Cyanine3-labeled goat anti-mouse IgG	Jackson ImmunoResearch	Cat#: 115-165-003; RRID:AB_2338680
Deposited data		
Mouse feces 16s ribosomal RNA gene amplicon sequencing data	NCBI Biosample	PRJNA892219
Mouse feces shotgun metagenome sequencing data	JGI IGM/M	Taxon ID 3300051405
Source code for the Shiny App visualizing the shotgun metagenomic analysis	https://github.com/connor-reid-tiffany/Metagenomics-of-Sorbitol-Intolerant-Mice	N/A
Shiny App visualizing the shotgun metagenomic analysis	https://clostridia-enjoyer.shinyapps.io/sorbitolMetagenome	N/A
Experimental models: Organisms/strains		
Mus musculus C57BL/6J	The Jackson Laboratory	Cat#: 000664
Mus musculus C57BL/6 *Pparg*$^{fl/fl}$*Villin*$^{cre/-}$	Bred in house[40]	N/A
Mus musculus C57BL/6 *Pparg* $^{fl/fl}$*Villin*$^{-/-}$	Bred in house[40]	N/A
Oligonucleotides		
5'-ACTCCTACGGGAGGCAGC-3'	Croswell et al.[75]	*Clostridia*: Forward
5'-GCTTCTTTAGTCAGGTACCGTCAT-3'	Croswell et al.[75]	*Clostridia*: Reverse
5'- TTCGRGACADKRGWGACAGGTGGT-3'	This study	*Anaerostipes: Forward*
5'- TGGGATTTGCYTMSYCTCACGAS-3'	This study	*Anaerostipes*: Reverse
5'-GTGCCAGCMGCCGCGGTAA-3'	Resendiz-Nava et al.[76]	*Enterobacterales: Forward*
5'-GCCTCAAGGGCACAACCTCCAAG-3'	Resendiz-Nava et al.[76]	*Enterobacterales: Reverse*
5'-CATTCATGGCCATATCAATGGAAT TTCCTGCAACTGCTG -3'	This study	srlAEB_EcN_AB_F
5'- TCATTTTTTACATTGTTCTCTCCTTCAGG -3'	This study	srlAEB_EcN_AB_R
5'- GAGAACAATGTAAAAAATGAATCAGGT TGCCGTTGTCATCG -3'	This study	srlAEB_EcN_CD_F
5'-GGAATTCATGCAGTTCACTTTGA GTCAGCCCGACGCCA-3'	This study	srlAEB_EcN_CD_R
5'-AAGTGAACTGCATGAATTC-3'	This study	pRE_linear_F
5'-CATTGATATGGCCATGAATG-3'	This study	pRE_linear_R
5'-TATCGATAAGCTTGATATCGGA ATTTCCTGCAACTGCTG-3'	This study	srlAEB_pcomp_up_F
5'-GGTTCACCTTCTTTAAATCCGTCGATAGC-3'	This study	srlAEB_pcomp_up_R
5'-GGATTTAAAGAAGGTGAACCCGCGGAGG-3'	This study	srlAEB_pcomp_down_F
5'-AGGGAACAAAAGCTGGAGCTGCG CCTAAGGTTTGCCCAC-3'	This study	srlAEB_pcomp_down_R
Software and algorithms		
Prism v8.0	GraphPad	N/A
NEBuilder Assembly Tool	https://nebuilder.neb.com/#!/	N/A
QIIME 1.8	Kuczynski et al.[77]	N/A
Trimmomatic v0.39	Bolger et al.[78]	N/A
DADA2 v1.18	Callahan et al.[79]	N/A
Phyloseq	McMurdie and Holmes[80]	N/A
DESeq2	Love et al.[81]	N/A
LEFSe galaxy server	Segata et al.[82]	N/A
Clustal Omega	Sievers and Higgins[83]	N/A
DEGEPRIME v1.1.0	Hugerth et al.[84]	N/A

(*Continued on next page*)

Continued

REAGENT or RESOURCE	SOURCE	IDENTIFIER
Metaspades v3.15.2	Nurk et al.[85]	N/A
BBMap	https://sourceforge.net/projects/bbmap/	N/A
R package Omu v1.0.6	Tiffany and Bäumler[86]	N/A
R package gplots v3.1.3	https://github.com/talgalili/gplots	N/A
R package ggplot2 v3.3.6	https://ggplot2.tidyverse.org	N/A
R package Shiny v 1.7.2	https://cran.r-project.org/web/packages/shiny/	N/A
Other		
Mouse 10 % Fat Diet	Teklad Diet	#TD110675
Mouse 45 % Fat Diet	Teklad Diet	#TD06415
Mouse 45 % Fat Diet with 5-ASA (0.125 %)	Teklad Diet	#TD 180827

RESOURCE AVAILABILITY

Lead contact

Further information and requests for resources and reagents should be directed to and will be fulfilled by the lead contact, Prof. Andreas Bäumler ajbaumler@ucdavis.edu

Materials availability

Reagents generated in this study are available, upon reasonable requests, with a completed material transfer agreement.

Data and code availability

Data: Raw sequencing reads for the 16S rRNA sequencing can be found on the NCBI: BioProject number [PRJNA892219] and are publicly available as of the date of publication. Reads for the shotgun metagenomic sequencing are publicly available as of the date of publication at the JGI IGM/M: taxon ID 3300051405.

Code: Source code for the Shiny App visualizing the shotgun metagenomic analysis can be found at https://github.com/connor-reid-tiffany/Metagenomics-of-Sorbitol-Intolerant-Mice, while the app itself is available at https://clostridia-enjoyer.shinyapps.io/sorbitolMetagenome/

Additional information: Any additional information required to reanalyze the data reported in this paper is available from the lead contact upon request.

EXPERIMENTAL MODEL AND STUDY PARTICIPANT DETAILS

Mouse Models

The Institutional Animal Care and Use Committee at the University of California at Davis approved all animal experiments in his study. Male C57BL6/J mice, aged 6 weeks were obtained from The Jackson Laboratory. C57BL/6 Pparg$^{fl/fl}$Villin$^{cre/-}$ and littermate Pparg $^{fl/fl}$Villin$^{-/-}$ mice were generated at UC Davis by mating Pparg$^{fl/fl}$ mice with Villin$^{cre/-}$ mice (The Jackson Laboratory). Animals were either fed a (sorbitol-free) 10 % control (LF) diet (Teklad Diet, #TD 11065) or (sorbitol-free) 45% fat (HF) diet (Teklad Diet, #TD06415) from weaning at the age of 6 weeks until the end of the experiment.

For experiments using a model of antibiotic-induced transient sorbitol intolerance, mice were maintained on a sorbitol-free low-fat diet and mock-treated or treated with single dose of 20 mg/animal streptomycin via oral gavage. One day or five days later, drinking water was supplemented with 5 % (w/v) D-sorbitol (Sigma Aldrich) solution for three days. In some experiments, mice were orally inoculated with different doses (between 10^0 and 10^9 cfu in a volume 100 μL) of *A.caccae* one day after streptomycin treatment. In some experiments, mice were orally inoculated with different doses (between 10^0 and 10^9 cfu in a volume of 100 μL) of either WT *Escherichia coli* strain Nissle 1917 or an isogenic strain deficient for sorbitol utilization (*srlAEB* mutant) one day after streptomycin treatment. After starting sorbitol supplementation in drinking water, body weights of mice were monitored daily, and the experiment was terminated 2 days after starting sorbitol supplementation. Fecal colonization of bacteria was determined by homogenizing feces in 1mL of sterile PBS, followed by serially diluting the samples and plating on LB plates containing appropriate antibiotics for *E. coli*. The colonization levels of *A. caccae* and were ascertained using qRT-PCR. For comparison, the colonization levels of *E. coli* were also ascertained using qRT-PCR.

For experiments using a model of prolonged sorbitol intolerance, mice maintained on a sorbitol free low-fat or high fat diet for 14 days were mock-treated or treated with a single dose of 20 mg/animal streptomycin via oral gavage. After maintaining mice

for four more weeks on the same diet, drinking water was supplemented with 5 % D-sorbitol solution for three days. For some experiments, mice were inoculated with 10^9 cfu of *Anaerostipes caccae*, *E. coli* Nissle 1917 or *Lactiplantibacillus plantarum strain* NCIMB8826-*R* in volume of 100 μL at the beginning of seven days of sorbitol exposure. After starting sorbitol supplementation in drinking water, body weights of mice were monitored daily, and the experiment was terminated three or seven days after starting sorbitol supplementation. For some experiments, mice received supplements of 5-aminosalicylic acid (5-ASA) at a dose of 1650 mg/kg/day (Teklad Diet, #TD 180827) mixed into high-fat diet chow or tributyrin (5 g/kg), administered via oral gavage over a seven-day period. For 5-ASA prophylaxis, mice were maintained on a low-fat or a high-fat diet for 14 days and were mock-treated or received a single dose of streptomycin (20 mg/mouse) via oral gavage, and high-fat diet chow was switched to a HF diet chow supplemented with 5-ASA for the remainder of the experiment.

Bacterial strains and culture conditions

The *E. coli* strains used in this study were routinely grown in LB broth (BD Bioscience) or on LB plates. The *L. plantarum* strain was grown in MRS (BD Bioscience) broth or on MRS plates. For animal experiments, bacterial cultures were grown overnight at 37°C in LB broth or MRS broth under aerobic conditions. 0.1 mg/mL of carbenicillin or 0.05 mg/mL of kanamycin or 0.05 mg/mL of rifampicin were added as required. For inoculating mice with different does of *A. caccae*, *A. caccae* strain was grown anaerobically in EG broth for 48 hours and 10 ml of overnight culture were spun down and pelleted at 4°C, then resuspended to a final concentration between $1x10^1$ and 10^{10} cfu/ml in fresh media.

Human studies

Banked fecal samples from a previous study were utilized to assess sorbitol dehydrogenase levels in human feces.[20] The study conformed to the Declaration of Helsinki's guidelines and received the necessary approvals from the Institutional Review Board of CHA Bundang Medical Center (protocol number: 2016-06-055) and Yonsei University College of Medicine (protocol number: 4-2015-0608). Subjects who met the ROME III criteria for IBS were enrolled between June 2016 and July 2017 at the Department of Family Medicine, CHAUM Hospital, Seoul, Korea. Healthy controls were recruited through advertisements and were required to complete a questionnaire to ensure they did not have any gastrointestinal symptoms. To further classify IBS patients, calprotectin levels in feces were determined using an ELISA. A questionnaire was used to determine intolerance to sugar-free foods or beverages, asking participants, "Does consuming sugar-free food or drinks with substitute/artificial sugar exacerbate your gastrointestinal symptoms?" Sorbitol dehydrogenase in feces was quantified using a sorbitol dehydrogenase assay kit, following the provided instructions.

METHOD DETAILS

Construction of E. coli Nissle 1917 ΔsrlAEB

A *srlAEB* mutant of *E. coli* Nissle 1917 was generated by allelic exchange. Approximately 500 bp upstream of *srlA* and 500 bp downstream of *srlB* (the flanking regions of the *srlAEB* operon) were amplified from genomic DNA using primers srlAEB_EcN_AB_F/R and srlAEB_EcN_CD_F/R (key resources table), respectively. PCR using genomic DNA as the template was carried out using Q5 Hot Start High-Fidelity 2X Master Mix (NEB) and amplification products were purified using the QIAquick PCR Purification Kit (Qiagen). The suicide vector pRE112[71] was linearized by PCR using the primers pRE_linear_F/R (key resources table). Primers used to amplify the flanking regions were designed to allow assembly of amplification products together with linearized pRE112 using the NEBuilder Assembly Tool (NEB). Linearized pRE112 and the amplified flanking regions of the *srlAEB* operon were assembled into a circularized plasmid using NEBuilder HiFi DNA Assembly Master Mix (NEB). Assembled candidate plasmids were transformed into *E. coli* strain S17-1 λ*pir*,[67] screened for correct insert size by colony PCR using MyTaq Red Mix (Meridian Bioscience). Assembled candidate plasmids were visualized by agarose gel electrophoresis, extracted using the QIAprep Spin Miniprep Kit (Qiagen), and submitted to the UC Davis DNA Sequencing Core for insert sequence verification. A clone with a sequence-verified insert was termed pAWLR80.

Plasmid pAWLR80 was conjugated into *E. coli* Nissle 1917 carrying the temperature-sensitive plasmid pSW172[72] for counter selection. Mating was performed overnight at 30°C and transconjugants were selected by plating on LB agar containing carbenicillin and chloramphenicol. Sucrose selection was then performed on agar plates containing 8 g/L nutrient broth base (Difco) and 5 % sucrose. Sucrose-resistant, chloramphenicol-sensitive clones were screened by colony PCR for the shortened allele of the *srlAEB* operon. Plasmid pSW172 was cured from resulting *srlAEB* deletion mutants by cultivating clones at 37°C and selecting for a carbenicillin-sensitive clone, which was termed AWLR133. Plasmid pCAL61[73] was electroporated into AWLR133 to introduce a selectable kanamycin marker.

Complementation of the srlAEB genes was accomplished by cloning them into the low-copy vector pWSK29.[74] The native promoter of the genes was maintained in the expression construct. The NEBuilder Assembly Tool (New England Biolabs) web application was used to generate primers for the amplification of the locus containing *srlAEB*, including 500 bp upstream of the *srlA* start codon, and 50 bp downstream of the *srlB* stop codon. To facilitate efficient amplification by PCR, the *srlAEB* locus was amplified in two fragments of equal length using genomic DNA as the template with the primers srlAEB_pcomp_up_F, srlAEB_pcomp_up_R, srlAEB_pcomp_down_F, and srlAEB_pcomp_down_R. Q5 Hot Start High-Fidelity 2X Master Mix (NEB) and amplification products were purified using the QIAquick PCR Purification Kit (Qiagen). Linearization of pWSK29 was carried out by restriction-digestion using EcoRI-HF (New England Biolabs) and SacI-HF (New England Biolabs). Linearized pWSK29 and the amplified *srlAEB* fragments

were assembled into a circularized plasmid using NEBuilder HiFi DNA Assembly Master Mix (NEB). Assembled candidate plasmids were transformed into *E. coli* strain DH5α λ*pir*,[66] and screened for correct insert size by colony PCR using MyTaq Red Mix (Meridian Bioscience). Assembled candidate plasmids were extracted using the QIAprep Spin Miniprep Kit (Qiagen), and submitted to Genewiz (Azenta Life Sciences) for whole plasmid sequencing. A sequence-verified clone was termed pAWLR169 and electroporated into *E. coli* Nissle 1917 *slrAEB*.

16S rRNA gene amplicon sequencing sample preparation, library preparation, and Sequencing

For 16S rRNA amplicon library preparation and sequencing, Primers 319F (**TCGTCGGCAGCGTCAGATGTGTATAAGAGACAG**(spacer)*GT*ACTCCTACGGGAGGCAGCAGT) and 806R(**GTCTCGTGGGCTCGGAGATGTGTATAAGAGACAG**(spacer)*CC*GGACTACNVGGGTWTCTAAT) were used to amplify the V3-V4 domain of the 16S rRNA using a two-step PCR procedure. In step one of the amplification procedures, both forward and reverse primers contained an Illumina tag sequence (bold), a variable length spacer (no spacer, C, TC, or ATC for 319F; no spacer, G, TG, ATG for 806R) to increase diversity and improve the quality of the sequencing run, a linker sequence (italicized), and the 16S target sequence (underlined). Each 25 μl PCR reaction contained 1 Unit Kapa2G Robust Hot Start Polymerase (Kapa Biosystems), 1.5 mM $MgCl_2$, 0.2 mM final concentration dNTP mix, 0.2 μM final concentration of each primer and 1μl of DNA for each sample. PCR conditions were; an initial incubation at 95°C for 3 min, followed by 25 cycles of 95°C for 45 seconds, 50°C for 30 seconds, 72°C for 30 seconds and a final extension of 72°C for 3 minutes. In step two, each sample was barcoded with a unique forward and reverse barcode combination using forward primers (**AATGATACGGCGACCACCGAGATCTACAC**NNNNNNNNTCGTCGGCAGCGTC) with an Illumina P5 adapter sequence (bold), a unique 8 nt barcode (N), a partial matching sequence of the forward adapter used in step one (underlined), and reverse primers (**CAAGCAGAAGACGGCATACGAGAT**NNNNNNNNGTCTCGTGGGCTCGG) with an Illumina P7 adapter sequence (bold), unique 8 nt barcode (N), and a partial matching sequence of the reverse adapter used in step one (underlined). The PCR reaction in step two contained 1 Unit Kapa2G Robust Hot Start Polymerase (Kapa Biosystems), 1.5 mM $MgCl_2$, 0.2 mM final concentration dNTP mix, 0.2 μM final concentration of each uniquely barcoded primer and 1ul of the product from the PCR reaction in step one diluted at a 10:1 ratio in water. PCR conditions were; an initial incubation at 95°C for 3 min, followed by 8 cycles of 95°C for 30 seconds, 58°C for 20 seconds, 72°C for 20 seconds and a final extension of 72°C for 3 minutes. The final product was quantified on the Qubit instrument using the Qubit Broad Range DNA kit (Invitrogen) and individual amplicons were pooled in equal concentrations. The pooled library was cleaned utilizing Ampure XP beads (Beckman Coulter) then the band of interest was further subjected to isolation via gel electrophoresis on a 1.5 % Blue Pippin HT gel (Sage Science). The library was quantified via qPCR followed by 300-bp paired-endvsequencing using an Illumina MiSeq instrument in the Genome Center DNA Technologies Core, University of California, Davis.

16S rRNA gene amplicon sequencing analysis

Sequencing reads were demultiplexed using QIIME 1.8,[77] and non-biological nucleotides were trimmed using Trimmomatic.[78] 16S rRNA sequencing reads were then processed and assembled into amplicon sequence variants (ASV) using dada2[79] in R (https://www.R-project.org/). First, reads with more than 2 expected errors were removed. Dereplication and sample inferences were then performed on forward and reverse reads, prior to merging. A sequence table was constructed from merged reads, and chimeric reads were subsequently removed. Taxonomy was assigned to reads to the species level using the dada2 formatted rdp training dataset 14 which can be found here: https://zenodo.org/record/158955#.XJqlnxNKjUI. The R package phyloseq[80] was then used in downstream analysis of the data, including the generation of a phyloseq object, relative abundance bar plots. Relative abundance boxplots were generated using ggplot2. For linear discriminant analysis, data transformed using the DESeq2[81] median of ratios method to account for differences in reads between samples, parsed, written to a tab separated text file, and then uploaded to the LEfSe[82] galaxy server where the default statistical parameters were used in the analysis to generate LDA scores and the LDA cladogram.

Shotgun Metagenome Data Analysis

Assembly, Annotation, and Binning

Metagenome QC and assembly was performed according to the workflow found in https://journals.asm.org/doi/10.1128/mSystems.00804-20 (Clum et al.[87]) with modifications for co-assembly to yield higher quality bins. Metaspades v3.15.2[85] was used to create a co-assembly. Once co-assembled, each of the sequencing FASTQ reads files from the individual samples were mapped to the co-assembly contigs with BBMap. The contigs and coverage information were then submitted to IMG/M for annotation and binning (Clum et al., 2021).

Generation of count matrices of genes

For the gene count matrices, a custom script was used to parse out the contig_ID, gene_start, gene_stop (gene positions on contig), and gene_attributes data for each gene in the GFF files that were created during annotation. The custom script then parsed out the contig_ID and read_start (read positions on contig) from each of the BBMap mapping files. For each mapping file, if the read_ start position was within any gene_start and gene_stop positions in the GFF files, then the read was counted as mapping to that gene and the gene attributes (cath_funfam, COG, EC, hypothetical, KO, pfam, SMART, superfamily, tigrfam, and/or tRNA IDs) from the GFF file were tallied. All gene counts were derived using medium and high-quality bins.

Clustering and Plots

Gene names and KEGG[29] orthology brite hierarchy metadata were assigned using the R package omu.[86] Heatmaps were constructed using the function heatmap.2 from the R package gplots. Read counts were normalized using the median of ratios method in DESeq2, and then transformed using the function ln(1+x) before clustering. The sample dendrogram was created using hierarchical clustering on Euclidean distances calculated between sample vectors, with a complete linkage approach.

Bar plots of gene counts by taxonomic group were generated using the raw counts and the R package ggplot2. The following R packages were used in order to develop the web application featuring the shotgun metagenomic data: shiny, bslib, shinywidgets, ggplot2, officer, thematic, colourpicker, reshape2 (http://www.jstatsoft.org/v21/i12/.), RColorBrewer, gplots, gridextra, cowplot, ggrepel, and ggplotify.

D-Sorbitol Measurements

To measure D-sorbitol levels in the murine cecum, cecal contents were homogenized in 1 mL of sterile PBS, centrifuged at 300 g for 10 min at 4 °C, and then the supernatants were filtered through a 10-kDa spin column (Biovision). D-Sorbitol concentrations were determined using a D-sorbitol assay kit (Biovision) according to the manufacturer's instruction. Spike/Recovery assay was performed for validating cecal contents in this assay and the calculated recovery range was 117.60 %.

Sorbitol Dehydrogenase Activity Measurements

To measure sorbitol dehydrogenase activity in the murine cecum, cecal contents were homogenized 1 mL of sterile PBS, centrifuged at 300 g for 10 minutes at 4°C. Sorbitol Dehydrogenase activity was determined using a Sorbitol Dehydrogenase (SDH) Assay Kit (LSBio) according to the manufacturer's instructions.

Fecal water content

To measure the fecal water content, fecal pellets were collected and weighed. Then, fecal pellets were dried in a 50°C oven for 24 hours to remove water contents and were then weighed again. The percentage of water contents was calculated.

Determining bacterial absolute abundance using quantitative real-time PCR

For measuring absolute copy numbers of *Clostridia*, *Enterobacterales*, or *Anaerostipes* 16S rRNA genes in the feces, fecal DNA was extracted using the DNeasy PowerSoil Pro kit (Qiagen) according to the manufacturer's instructions. Real-time PCR was performed using SYBR-Green (Applied Biosystems) and class-specific (for *Clostridia*),[75] *Enterobacterales*-specific primers[76] or genus-specific (for *Anaerostipes*) primers (key resources table) at a final concentration of 0.25 mM. To create Genus specific primers to target *Anaerostipes spp.*, a custom script was written to gather all 16S genes from *Anaerostipes* isolates on the NCBI. Entrez direct was used to gather accessions from all *Anaerostipes* isolates on NCBI into a text file which was then parsed using a custom script, and NCBI datasets was then used to gather the genes associated with those accessions. A multiple sequence alignment was then created using clustal omega.[83] The alignment was then used to generate primers with the software DEGEPRIME,[84] with a degeneracy score of 56 and length of 24 as parameters. The forward and reverse primers were chosen from hypervariable region 7 of the 16S gene to avoid hybridization to other *Lachnospiraceae* bacteria. We downloaded all *Clostridia* genomes from the NCBI, made a local BLAST database, and verified *in silico* that the primers do not hybridize to other *Clostridia*. In-sillico hybridization from DEGEPRIME showed 98.3 % and 100 % hybridization across *Anaerostipes* 16S rRNA genes for the forward and reverse primers, respectively. The amplicon generated by the primers has a length of 221 base pairs.

To generate plasmid standards, PCR was performed using a thermocycler with class-specific (for *Clostridia*) or genus-specific (for *Anaerostipes*) primers (key resources table). The PCR was confirmed by gel electrophoresis, and the PCR product was then purified using a DNA clean-up kit (Zymo Research) according to the standard kit protocol with no modifications. Following purification, the PCR product was then ligated into a linear TOPO-TA cloning vector, using a TOPO-TA cloning kit (Invitrogen). After ligation, the construct was transformed into chemically competent *Escherichia coli* TOP10 cells provided with the kit and cultured for approximately 1 hour in LB broth at 37°C. The cells were then plated on LB Agar plates with X-Gal (5-Bromo-4-Chloro-3-Indolyl β-D-Galactopyranoside) and Kanamycin to select colonies which kept the plasmid. A miniprep using a Qiaprep spin mini-prep kit was performed on a pure liquid culture from a single colony isolate to extract plasmid DNA. The plasmid DNA product was then linearized using the restriction enzyme BamHI (New England Biolab) according to manufacturer protocol. The linear plasmid DNA was quantified using a nanodrop and diluted to create a stock standard with 10^{10} copies of the 16S rRNA amplicon insert for use in qRT-PCR.

To calculate absolute copy numbers, a standard curve ranging from 10^1 to 10^{10} copies/mL of plasmid carrying a cloned 16S rRNA gene diluted in a 0.02 mg/mL of yeast RNA (Sigma Aldrich) was generated.

In vitro measurement of sorbitol in E. coli culture supernatants

The *in vitro* utilization of sorbitol by *E. coli* strains was assessed using M9 minimal medium (12.8 g/L Na_2HPO_4 $7H_2O$, 3 g/L KH_2PO_4, 0.5 g/L NaCl, and 1 g/L NH_4Cl), supplemented with 1 mM $MgSO_4$, 0.1 mM $CaCl_2$, 0.1% casamino acids, and 0.5% (w/v) D-sorbitol.

20 μL of an overnight culture of each *E. coli* strain containing 10^{10} CFU/mL were used to inoculate into 2 mL of M9 minimal medium containing D-sorbitol. The cultures were then incubated at 37°C overnight. Sorbitol concentrations were quantified in the cell culture supernatant using a D-sorbitol colorimetric assay kit.

In vitro growth assay of Clostridia strains

To determine the ability of *A. caccae* and *E. asparagiforme* to utilize sorbitol as a carbon source *in vitro*, no carbon defined media (NCDM), which is a modified form of non-carbon minimal media[88] supplemented with 5 % (v/v) ATCC Vitamin Supplement (ATCC), 2 % (v/v) ATCC Trace Mineral Supplement (ATCC), Bacto Casamino acids (4.575 g/L) (ThermoFisher), cysteine (400 mg/L) (Sigma-Aldrich), methionine (27 mg/L) (Sigma-Aldrich), alanine (72 mg/L) (Sigma-Aldrich), tryptophan (30 mg/L) (Sigma-Aldrich) and Vitamin K2 (72 mg/L) (Sigma-Aldrich) was used. Glucose or D-sorbitol was used as a carbon source at a final concentration of 0.5% (w/v). Individual strains were grown in the anaerobic chamber in 2 mL of NCDM containing glucose for 24 hours. Then, the culture was spun down at 12,500 rpm for 3 minutes and the pellets were resuspended in 750 μL of reduced sterile PBS. 25 μL of resuspended pellet was inoculated into 2mL of NCDM containing glucose, D-sorbitol, or no added carbohydrates and incubated at 37°C for 72 hours. The growth of bacteria was determined by serially diluting the cultures and plating on plates of EG.

Hypoxia staining and imaging

Mice were injected intraperitoneally with 100 mg/kg of pimonidazole HCl (Hypoxyprobe) in PBS sixty minutes before necropsy. The staining procedure with the Hypoxyprobe kit was conducted as detailed in prior studies.[20] Paraffin-embedded tissues were mounted on slides and prepared for staining: they were treated with xylene twice for 10 minutes each and then with ethanol for 3 minutes in sequences of 95 %, 80 %, and 70 %. Samples were treated with 20 mg/mL Proteinase K in TE buffer at 37°C for 15 minutes. Nonspecific binding sites were blocked using serum at room temperature for an hour, followed by an overnight stain at 4°C using the mouse IgG1 anti-PMDZ monoclonal antibody 4.3.11.3 (Hypoxyprobe). The slides were then subjected to a 90-minute stain at room temperature with Cyanine3-labeled goat anti-mouse IgG (Jackson ImmunoResearch). Between each staining phase, slides were washed thrice in PBS for 5 minutes each. After the final wash, slides were briefly air-dried and mounted using Shandon Immu-Mount (Thermo Scientific). For imaging, the image numbers were randomized and blinded. Three representative images from each sample were captured using a Carl Zeiss AxioVision microscope equipped with AxioVision 4.8.1 software (Zeiss) at 20X for scoring and 63X for detailed imagery. Using ImageJ (NIH), the Texas Red channel (linked to Cyanine3) was singled out. From each image, three representative slices, each of the same size and containing the epithelial-lumen border, were saved. The Plot Profile for each slice was then determined. After unblinding, PMDZ peaks from each image were aligned, and the profiles for the 9 slices associated with each mouse were averaged, producing an average PMDZ Plot Profile and PMDZ Peak for every mouse.

Butyrate analysis

Approximately 100mg of cecal contents per mouse were collected in 200 μL PBS. Samples were vortexed to disrupt particulate matter and then centrifuged at 6,000 g for 10 min to pellet any remaining debris. For each sample, 100 μL of supernatant was combined with 10 μL of a solution containing deuterated acetate, propionate, and butyrate so that each deuterated metabolite was at a final concentration of 100 μM. Samples were dried without heat in a vacuum dryer and then stored at -80°C until use. Dried extracts were then solubilized by sonication in 0.1 ml anhydrous pyridine and then incubated for 20 min at 80°C. An equal amount of N-tert-butyldimethylsilyl-N-methyltrifluoroacetamide with 1% tert-butyldimethylchlorosilate (Sigma-Aldrich) was added, and the samples were incubated for 1 h at 80°C. Samples were centrifuged at 20,000 g for 1 min to remove leftover particles. One hundred microliters of the supernatant were transferred to an autosampler vial and analyzed by gas chromatography-mass spectrometry (Agilent 8890 Gas Chromatograph and Agilent 7000D Mass spectrometer). 1 μL of the sample was injected with a 1:50 split ratio at an injection temperature of 250°C on an HP 5ms Ultra Inert (2x15-m-length, 0.25-mm diameter, 0.25 μm film thickness) fused silica capillary column. Helium was used as the carrier gas with a constant flow of 1.2 mL/min. The gas chromatograph (GC) oven temperature started at 50°C for 20 min, rising to 90°C at 10°C/min and holding for 1 min, then raised to 310°C at 40°C/min with a final hold for 2 min. The interface was heated to 300°C. The ion source was used in electron ionization (EI) mode (70 V, 150 μA, 200°C). The dwell time for selected ion monitoring (SIM) events was 50 ms. Both acetate, propionate and butyrate were quantified using SIM. Efficient recovery of target metabolites was determined using deuterated compounds as internal standards. Quantification was based on external standards comprised of a series of dilutions of pure compounds, derivatized as described above at the same time as the samples.

QUANTIFICATION AND STATISTICAL ANALYSIS

Ratio's (fold increases or percentages) were transformed logarithmically before analysis to normalize the data. Bacterial numbers were transformed logarithmically before analysis. An unpaired Student's t test (for comparing two groups) or one-way ANOVA followed by Tukey's multiple-comparison test (for comparing more than two groups) were used to determine the differences among groups and two-way ANOVA followed by Tukey's multiple-comparison test were performed to determine the differences among the groups and period. To compare peak pimonidazole staining intensities, a Kruskal–Wallis test was performed. We performed all statistical analyses using the GraphPad Prism 8.0 Software. Statistical significance was defined as $P < 0.05$.

Microbiota profiling and metagenomic analysis

For linear discriminant analysis, data transformed using the DESeq2[81] median of ratios method to account for differences in reads between samples, parsed, written to a tab separated text file, and then uploaded to the LEfSe[82] galaxy server where the default statistical parameters were used in the analysis to generate LDA scores and the LDA cladogram.

Differential gene abundances were calculated using DESeq2 on reads normalized by the median of ratios method. A paired-sample wald test with a parametric fit was performed to obtain *P* values, which were then corrected to account for the false discovery rate using the Benjamini-Hochberg procedure. A significance threshold of 0.05 on the FDR corrected *P* values was used to determine significance. Confidence intervals were calculated using the following formula in R $\log_2$(fold-change) + qnorm(0.025)*lfcSE and $\log_2$(fold-change) - qnorm(0.025)*lfcSE, for upper and lower bounds respectively, where $\log_2$(fold-change) is the log base 2 of the fold change between groups, qnorm is a function to compute probabilities from known bounding values, and lfcSE is the log fold change standard error calculated when performing the DESeq2 model. Volcano plots, dot plots, and confidence interval of the $\log_2$(fold-change) plots were generated using the R package ggplot2 (https://ggplot2.tidyverse.org.)

ADDITIONAL RESOURCES

Description: URL

The web application (https://clostridia-enjoyer.shinyapps.io/sorbitolMetagenome/) allows interactive analysis of all KEGG orthology pathways within our metagenomic dataset.

CellPress
OPEN ACCESS

Supplemental figures

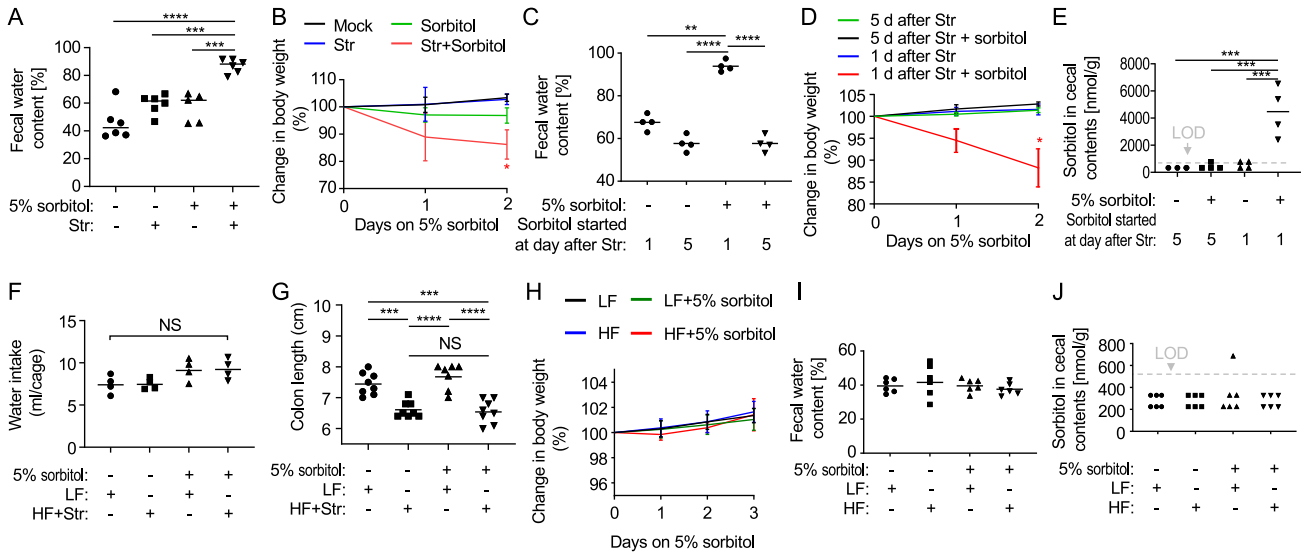

Figure S1. Streptomycin treatment causes transient sorbitol intolerance, whereas high fat intake does not induce sorbitol intolerance in the absence of antibiotic treatment, related to Figure 1

Mice fed a low-fat diet (10% fat) were mock-treated or treated with a single dose of streptomycin (Str) to generate sorbitol intolerance.

(A–E) Supplementation of drinking water with 5% sorbitol was started 1 day after streptomycin treatment (A and B) or at the indicated later time points after streptomycin treatment (C–E). (A) Fecal water content was determined after 2 days of sorbitol supplementation. (B) Change in body weight was monitored over time. Stars indicate significate decrease in weight compared with sorbitol only group. (C) Fecal water content was determined after 2 days of sorbitol supplementation. (D) Change in body weight after the beginning of sorbitol supplementation was monitored over time. Stars indicate significate decrease in weight compared with sorbitol only group. (E) The sorbitol concentration in cecal contents was measured by a colorimetric assay after 2 days of sorbitol supplementation.

(F and G) Mice maintained on a low-fat (LF) diet or a high-fat (HF) diet for 14 days were mock-treated or received a single dose of streptomycin (Str) by oral gavage. After maintaining mice for 4 more weeks on the same diet, mice received drinking water supplemented with 5% sorbitol for 3 days. (F) Water intake per cage was determined for each group during the period of sorbitol supplementation. (G) Colon length was determined at necropsy.

(H–J) Mice maintained on a low-fat (LF) diet or a high-fat (HF) diet for 42 days received normal drinking water or drinking water supplemented with 5% sorbitol for 3 days. (H) Change in body weight was monitored during sorbitol supplementation. (I) Fecal water content was determined after 3 days of sorbitol supplementation. (J) The sorbitol concentration in cecal contents was measured by a colorimetric assay after 3 days of sorbitol supplementation. (E and J) A gray dashed line indicates the limit of detection (LOD). *$p < 0.05$; ***$p < 0.005$; ****$p < 0.001$. p values were calculated by one-way ANOVA followed by Tukey's multiple-comparison tests (A, C, E–G, I, and J) or two-way ANOVA followed by Tukey's multiple-comparison tests (B, D, and H). (B, D, and H) Error bars represent standard deviation.

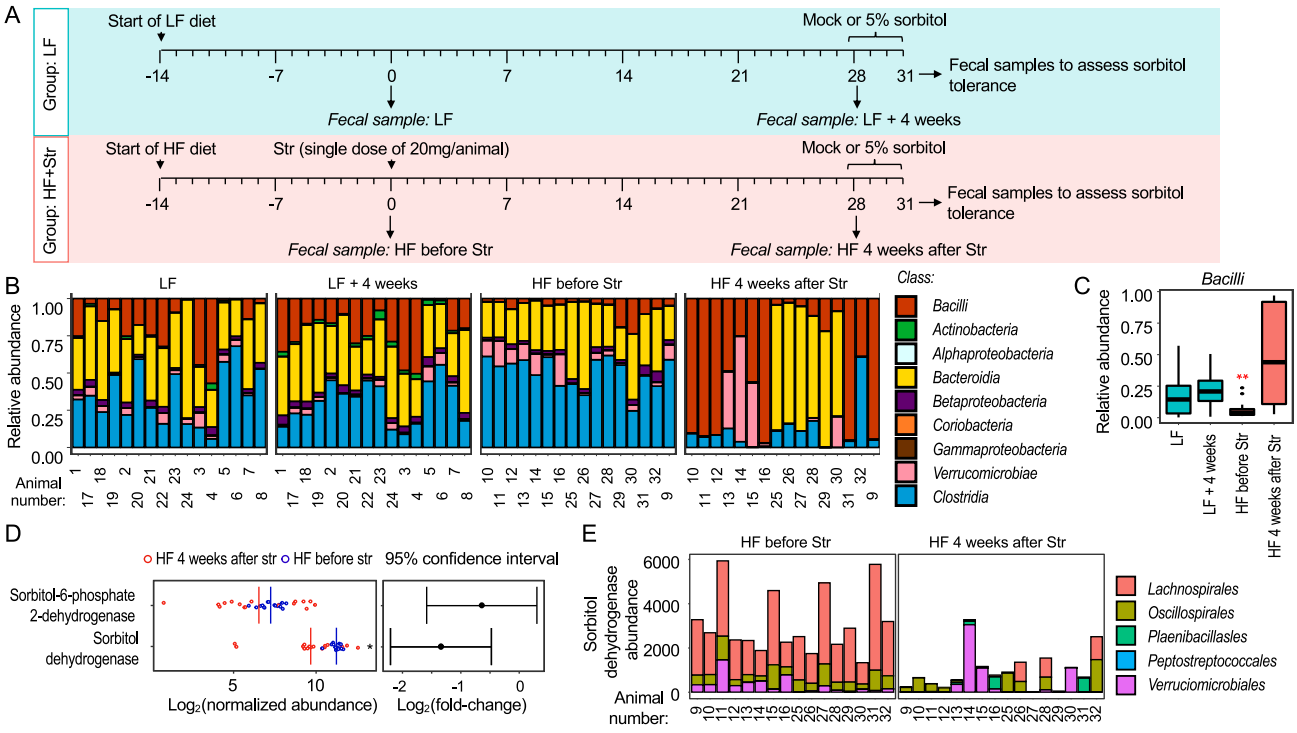

Figure S2. Compositional and functional changes in the microbiota of mice with prolonged sorbitol intolerance, related to Figure 2

Mice were maintained on a low-fat (LF) diet or a high-fat (HF) diet for 14 days. Fecal samples were collected (LF or HF before Str), and mice were mock-treated or received a single dose of streptomycin (Str) by oral gavage. After maintaining mice for 4 more weeks on the same diet, a second fecal sample was collected for analysis (LF + 4 weeks or HF 4 weeks after Str).

(A) Schematic showing experimental groups and time points of sample collection.

(B) Relative abundance of taxa (class level) in fecal samples collected from individual mice at the indicated time points.

(C) Box blots show the relative abundance of amplicon sequence variants (ASVs) belonging to the class *Bacilli*. The boxplots represent the first to third quartiles, and the line indicates the median value.

(D) The panel on the left shows the normalized abundance of sorbitol dehydrogenase or sorbitol-6-phosphate 2-dehydrogenase encoding sequences in samples collected prior to streptomycin treatment (blue circles) or 4 weeks after streptomycin treatment (red circles). Each circle denotes data collected from one animal. The panel on the right shows the 95% confidence interval for data displayed in the left panel.

(E) Abundance of genes encoding sorbitol dehydrogenase in samples collected prior to streptomycin treatment (HF before Str, left) or 4 weeks after streptomycin treatment (HF 4 weeks after Str, right). Colors denote the taxa (order level) to which gene sequences were assigned. *$p < 0.05$; **$p < 0.01$. p values were calculated by Kruskal-Wallis test (C) or by paired DESeq2 Wald test (E).

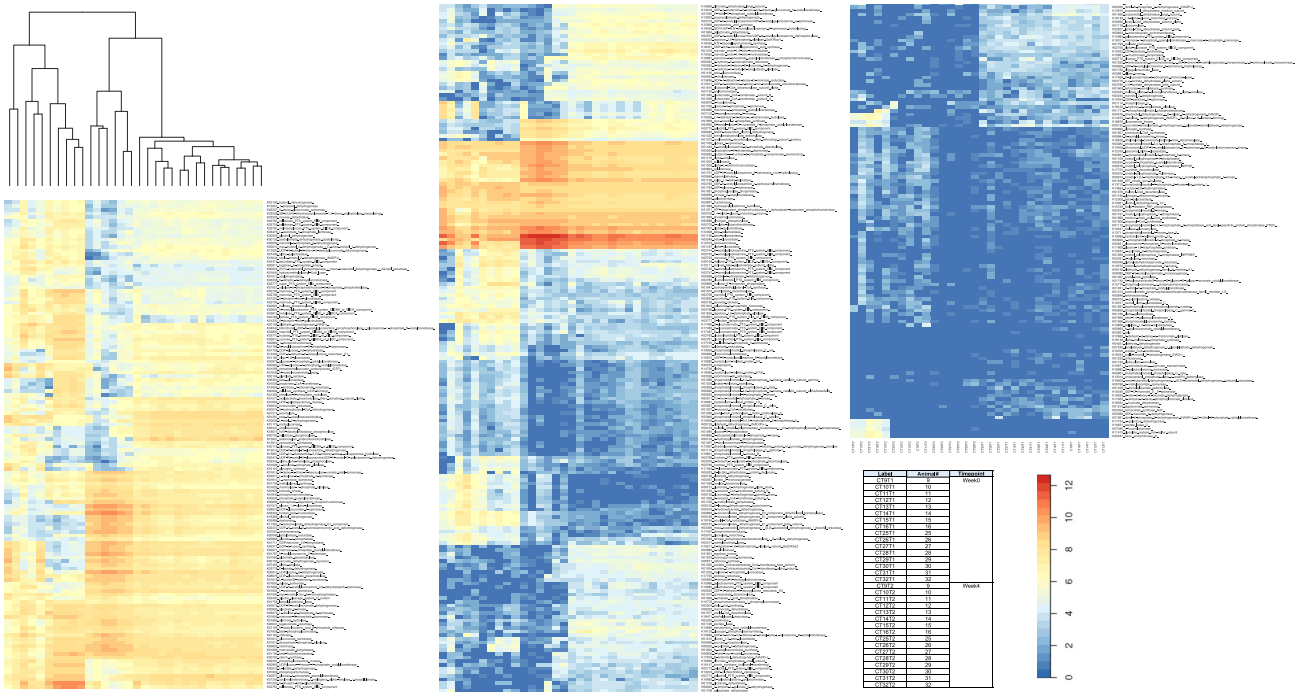

Figure S3. A history of antibiotic treatment and high fat intake changes the abundance of genes involved in carbohydrate catabolism in the fecal microbiota, related to Figure 2

Feces were collected from mice maintained on a high-fat (HF) diet for 14 days. Mice then received a single dose of streptomycin (Str) by oral gavage. After maintaining mice on an HF diet for 4 more weeks, feces were collected for analysis. DNA isolated from fecal samples collected before streptomycin treatment (HF before Str) and 4 weeks after streptomycin treatment (HF 4 weeks after Str) were subjected to metagenomic analysis. The graph shows a heatmap of changes in the abundance of genes involved in carbohydrate catabolism. Colors indicate increased abundance (red) or reduced abundance (blue) of genes 4 weeks after streptomycin treatment (HF 4 weeks after Str) compared with prior antibiotic exposure (HF before Str). Hierarchical clustering of samples is indicated above the graph.

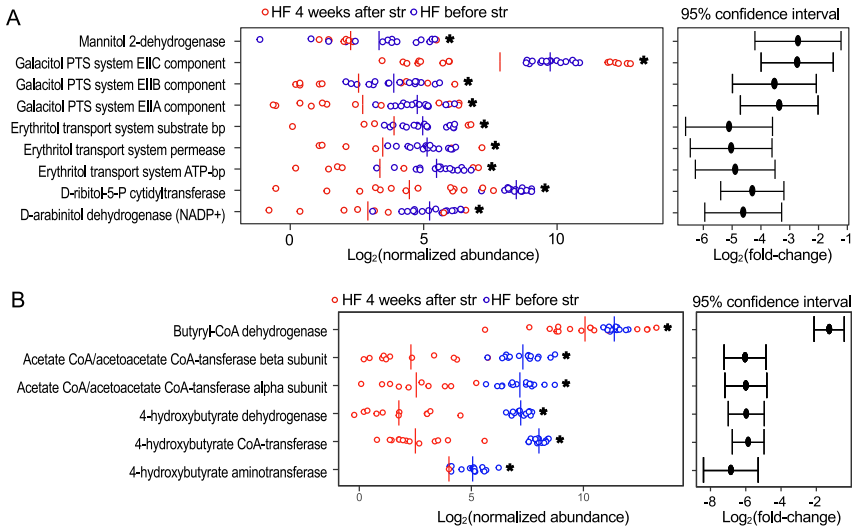

Figure S4. A history of antibiotic treatment and high fat intake reduces the abundance of genes involved in polyol catabolism and butyrate metabolism in the fecal microbiota, related to Figure 2

Feces were collected from mice maintained on a high-fat (HF) diet for 14 days. Mice then received a single dose of streptomycin (Str) by oral gavage. After maintaining mice on an HF diet for 4 more weeks, feces were collected for analysis. DNA isolated from fecal samples collected before streptomycin treatment (HF before Str) and 4 weeks after streptomycin treatment (HF 4 weeks after Str) were subjected to metagenomic analysis.

(A and B) The left panel shows the normalized abundance of genes encoding the indicated enzymes involved in polyol catabolism (A) or butyrate metabolism (B) in samples collected prior to streptomycin treatment (blue circles) or 4 weeks after streptomycin treatment (red circles). Each circle denotes data collected from one animal. The right panels show the 95% confidence interval for data displayed in the left panels. *$p < 0.05$ by paired DESeq2 Wald test.

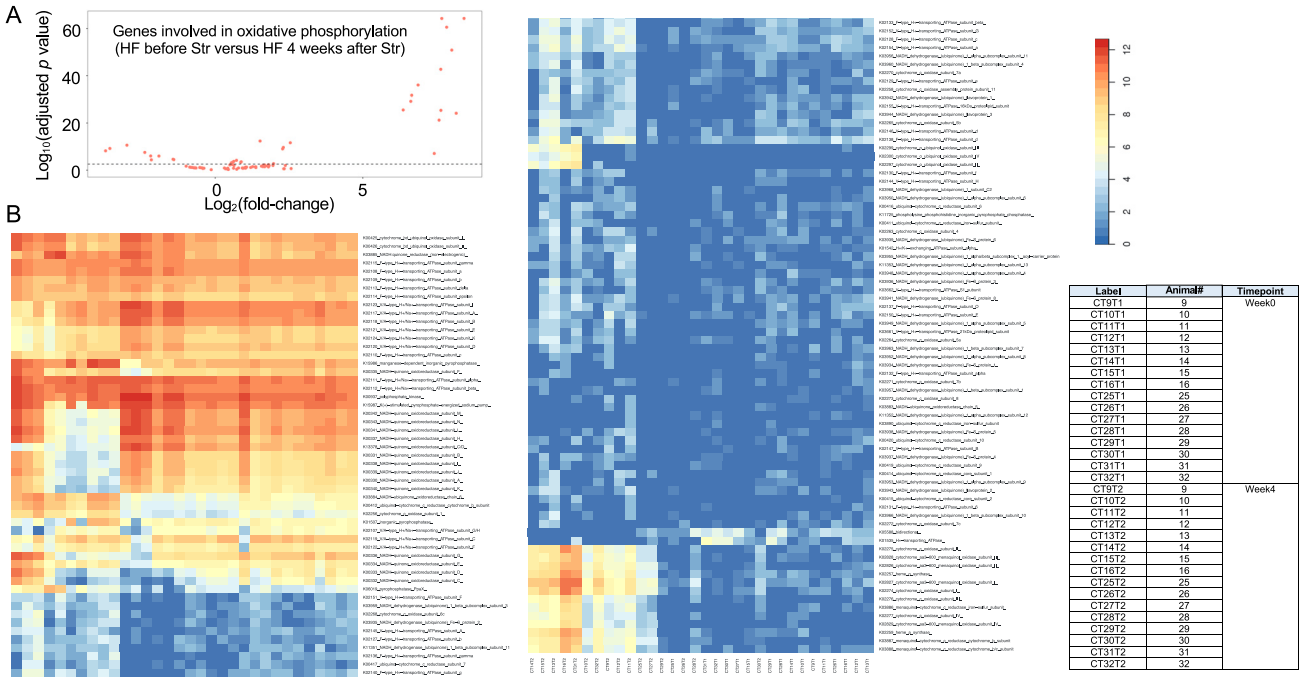

Label	Animal#	Timepoint
CT9T1	9	Week0
CT10T1	10	
CT11T1	11	
CT12T1	12	
CT13T1	13	
CT14T1	14	
CT15T1	15	
CT16T1	16	
CT25T1	25	
CT26T1	26	
CT27T1	27	
CT28T1	28	
CT29T1	29	
CT30T1	30	
CT31T1	31	
CT32T1	32	
CT9T2	9	Week4
CT10T2	10	
CT11T2	11	
CT12T2	12	
CT13T2	13	
CT14T2	14	
CT15T2	15	
CT16T2	16	
CT25T2	25	
CT26T2	26	
CT27T2	27	
CT28T2	28	
CT29T2	29	
CT30T2	30	
CT31T2	31	
CT32T2	32	

Figure S5. A history of antibiotic treatment and high fat intake reduce the abundance of genes involved in oxidative phosphorylation in the fecal microbiota, related to Figure 2

Feces were collected from mice maintained on a high-fat (HF) diet for 14 days. Mice then received a single dose of streptomycin (Str) by oral gavage. After maintaining mice on an HF diet for 4 more weeks, feces were collected for analysis. DNA isolated from fecal samples collected before streptomycin treatment (HF before Str) and 4 weeks after streptomycin treatment (HF 4 weeks after Str) were subjected to metagenomic analysis.

(A) Volcano plot of genes involved in oxidative phosphorylation.

(B) Heatmap of changes in the abundance of genes involved in oxidative phosphorylation. Colors indicate increased abundance (red) or reduced abundance (blue) of genes 4 weeks after streptomycin treatment (HF 4 weeks after Str) compared with prior antibiotic exposure (HF before Str).

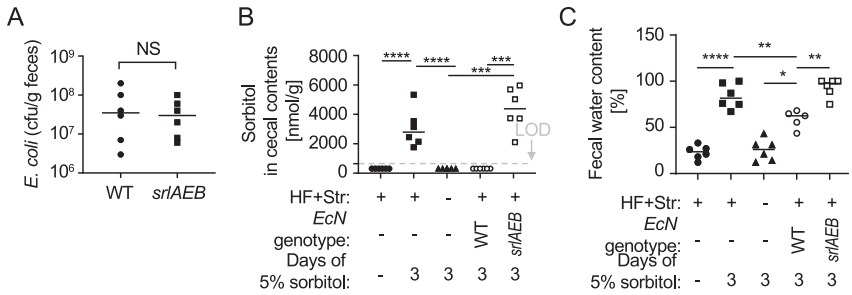

Figure S6. The ability to catabolize sorbitol is required by *E. coli* Nissle 1917 to protect against prolonged sorbitol intolerance, related to Figure 4

Mice reared and maintained throughout the experiment on a low-fat (LF) or a high-fat (HF) diet were mock-treated or received a single dose of streptomycin (Str), respectively. 4 weeks later, mice received drinking water supplemented with 5% sorbitol and were inoculated with 10^9 colony-forming units (CFUs) of *E. coli* Nissle 1917 (*EcN*) or an *E. coli* Nissle 1917 *srlAEB* mutant (EcN *srlABE*).

(A) Colony-forming units (CFUs) of *E. coli* were determined in the feces.

(B) The sorbitol concentration in cecal contents was measured by a colorimetric assay.

(C) Fecal water content was determined in feces. *$p < 0.05$; **$p < 0.01$; ***$p < 0.005$; ****$p < 0.001$. p values were calculated by Student's t test (A) or one-way ANOVA followed by Tukey's multiple-comparison tests (B and C). A gray dashed line denotes the limit of detection (LOD).

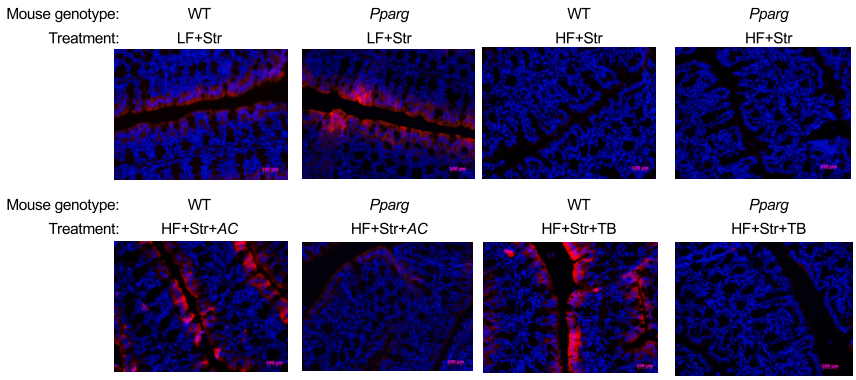

Figure S7. Butyrate and *A. caccae* restore epithelial hypoxia by stimulating epithelial PPAR-γ signaling, related to Figure 6I

Pparg$^{fl/fl}$*Villin*$^{cre/-}$ mice (*Pparg*) or *Pparg*$^{fl/fl}$*Villin*$^{-/-}$ littermate control mice (WT) reared and maintained throughout the experiment on a low-fat (LF) or a high-fat (HF) diet received a single dose of streptomycin (Str). 4 weeks later, mice received drinking water supplemented with 5% sorbitol and were inoculated with *A. caccae* (*AC*) or received supplementation with or tributyrin (TB). Samples were collected after 7 days of sorbitol supplementation. Mice were injected with pimonidazole before euthanasia. To stain hypoxic tissue, binding of pimonidazole (PMDZ) was detected using hypoxyprobe-1 primary antibody and a Cy-3 conjugated goat anti-mouse secondary antibody (red fluorescence) in sections of the colon that were counter stained with DAPI nuclear stain (blue fluorescence). Representative images for each group are shown.